Development and validation of a probe to measure meat quality

Project code:	2013/9501
Prepared by:	Stephanie Fowler, Dr Remy van de Ven and Dr David Hopkins NSW DPI
Date Published:	September 2015
Published by:	Australian Meat Processor Corporation

1. Executive Summary

Carcase assessment is a constant challenge for red meat processors, as lamb carcasses are only commonly assessed for market suitability on weight, sex and fat score. While informative for meat yield, these attributes are variable and may not be indicative of eating quality characteristics, such as tenderness. Consequently, better carcase assessment methods are required by the sheep meat industry. This report describes an investigation into the development and validation of one optic technology; a Raman spectroscopic hand held device for the assessment of meat quality of commercial lamb processed in Australia.

Spectra were collected at 25 minutes, 24 hours and 5 days post mortem (PM) using a hand held Raman device. The spectra were regressed against shear force values and traditional indicators of meat quality including pH values, cooking loss, purge, colour, sarcomere length, particle size, intramuscular fat levels and major fatty acid group concentrations using partial least squares.

The best prediction of shear force values at 5 days PM in the *m. semimembranosus* (SM) was found using spectra collected 24 h (R^2_{cv} = 0.27), however the prediction of shear force was inconsistent over time as further experiments did not demonstrate the ability to predict shear force values in the same muscle or the **m. longissimus lumborum**. Therefore, this research indicates that prediction of shear force of fresh intact lamb using Raman spectroscopy does not have the repeatability and robustness required by industry at this time.

Models for the prediction of other meat quality traits suggested that there was an ability to predict pH measured at 24 hours (pH_{24}) and purge using spectra measured pre-rigor (R^2_{cv} = 0.27 and 0.32) and pHu, purge and L* (meat lightness) values from spectra measured at 24 hours PM(R^2_{cv} = 0.22 – 0.59). Consequently, it is hypothesised that Raman spectroscopy is able to predict meat quality traits which relate to early PM metabolism. However, spectra underlying these predictions were complex and due to overlapping signals from compounds with similar chemical composition it was not possible to determine the biochemical compounds which contribute to these predictions.

Predictions of the major fatty acid groups were the most promising, yielding coefficients of determination coefficients (r^2) of 0.93 – 0.54 and reductions in error of up to 7.8% for the prediction of polyunsaturated (PUFA) and monounsaturated (MUFA) fatty acids, as well as saturated fatty acids, which had been adjusted for the level of intramuscular fat (IMF). However, there may be some overlap in Raman signals arising from the head groups of phospholipids, which may be causing a reduction in the accuracy when cross validation is used to determine the robustness of the prediction. Hence, further research needs to determine the impact of various lipid conformations on the prediction of major fatty acid groups in fresh intact muscle.

Overall, this study suggests that with further development to the Raman spectroscopic hand held device it may be possible to predict properties of meat which are associated with more than one biochemical characteristic or identify carcasses which deviate from normal post mortem metabolic processes, resulting in increased purge or low pHu values, using a single non-invasive measurement.

Table of Contents

2. Background

Due to advances in meat grading systems, there has been an increased focus in recent years on the meat product quality characteristics required to meet consumer preferences. However, as lamb carcasses are commonly assessed for market suitability using only weight, age, sex and fat scores, which may not be indicative of quality, better carcase assessment tools are required for prime lamb processors.

Although laboratory methods for measuring indicators of eating quality have been well established, methods such as measurement of shear force, sarcomere length and particle size are labour and time intensive as well as destructive. Consequently, alternative methods including nuclear magnetic resonance (NMR), ultrasound, impedance and computerised tomography (CT) have been investigated as potential tools for carcase assessment.

Of the technologies which have been investigated to measure carcase quality, optic technologies are of particular interest for adoption in commercial situations as recent developments in digital camera and laser technologies have facilitated the development of components that are suited to portable devices (Damez & Clerjon, 2008). Hence, optic technologies are ideal for use in commercial operations as they overcome the limitations associated with other technologies because they are non-destructive and do not require sample preparation or bulky equipment (Damez & Clerjon, 2008).

Raman spectroscopy (RS) is one such optic technology which uses scattering of light to provide information on the chemical composition of matter (Das & Agrawal, 2011). Unlike near infra-red (NIR) spectroscopy, RS is not affected by varying water content and is therefore suited to the measurement of meat and muscle foods (Herrero, 2008b). Research in meat science has not overlooked its potential and preliminary studies conducted using the technology have suggested that RS is capable of predicting sensory traits in beef silverside (Beattie *et al.*, 2004b) and the effects of ageing in pork *m. longissimus dorsi* (Beattie et al., 2008) with good accuracy ($R^2 = 0.62 – 0.71$). However, the commercial application of these preliminary studies is limited due to the size, weight and power consumption of the lasers in the bench top Raman devices used (Schmidt *et al.*, 2009).

Schmidt *et al.* (2009) overcame the limitations of the bench top devices by miniaturising them and combining the laser, filters and mirrors into one module making it ideal for *in-situ* measurements. A preliminary investigation of the Raman hand held device indicated that it was able to predict the shear force value of lamb ***m. longissimus lumborum*** with good accuracy ($R^2 = 0.79$ and $R^2 = 0.86$ for two data groups). However, as the samples were frozen and thawed for logistical reasons the application of this finding to industry is limited. Consequently, this project was undertaken to investigate the potential of the Raman hand held device to predict the meat quality traits of fresh intact lamb.

3. Project Objectives

1. Establish whether measurement of sheep meat at 1 day post mortem using a Raman hand held probe is useful for predicting shear force after an ageing period of 5 days.

2. Establish whether the probe can be used to predict shear force of 5 day aged meat.

3. Establish what biochemical and biophysical changes the probe is detecting in relation to tenderisation and to explore the potential of the probe to provide measures of other traits such as fatty acids and intramuscular fat.

3.1 Objectives 1 & 2

1. Establish whether measurement of sheep meat at 1 day post mortem using a Raman hand held probe is useful for predicting shear force after an ageing period of 5 days.

2. Establish whether the probe can be used to predict shear force of 5 day aged meat.

3.1.1 Introduction

Although tenderness may not be as significant in determining the eating quality of lamb in comparison to other sensory qualities, tough lamb is still associated with a poor eating experience for the consumer (Thompson *et al.*, 2005b). Due to the number of factors which impact on the tenderness and eating quality of red meats, it is unsurprising that much research has concentrated on technologies which may have the potential to objectively measure tenderness.

Raman spectroscopy has several distinct advantages for online measurement of meat products as it is non-destructive, not effected by varying water content and is not based on the absorption of light (Yang & Ying, 2011). Meat science research has not overlooked these advantages and studies have revealed RS is able to explain variation in shear force with a correlation coefficient (R^2) equal to 0.77 for pork (Beattie *et al.*, 2008) and predict sensory traits of cooked beef silverside (Beattie *et al.*, 2004b). However, the Raman bench top device that was used for these studies is not suitable for industrial application and the integration times used are too long for online scenarios. Alternatively, Schmidt *et al.* (2013) reported that Raman spectra taken with a hand held device enabled the prediction of shear force values of lamb *m. longissimus thoracis et lumborum* ($R^2 = 0.79$ and 0.86 for two sample groups), although these samples were frozen and thawed. A further study by Bauer *et al.* (2013) demonstrated the potential of the same hand held Raman device to predict shear force values of aged bovine *m. gluteus medius muscles* ($R^2 = 0.87$).

The conversion of muscle to meat causes several changes in structure which are critical in determining eating quality, the first of which occurs at slaughter when the oxygen source to the muscle is terminated. Consequently, the muscles undergo a series of biochemical reactions which result in the muscle entering *rigor mortis* which is characterised by muscle inextensibility (Tornberg, 1996). Furthermore, post *rigor* tenderisation may also be affected by the metabolic processes which occur during this early PM period, as higher carcase temperatures at *rigor* have been associated with greater rates of proteolysis (Koohmaraie *et al.*, 1988). Hence, indicators of lamb meat quality, including pH, sarcomere length and particle size are commonly measured at approximately 24 h PM (Hopkins *et al.*, 2011b) once most of the biochemical and biophysical changes associated with the on-set of *rigor* have occurred (Savell *et al.*, 2005).

Further changes to meat quality occur during PM storage because proteolysis which occurs during ageing degrades the myofibrils increasing tenderness (Hedrick *et al.*, 1993, Thompson *et al.*, 2005b, Bekhit *et al.*, 2007). While the improvements to tenderness as a result of proteolysis are widely accepted, the proteins which degrade and the mechanisms responsible are still not totally clear (Takahashi, 1996, Hopkins & Thompson, 2002, Koohmaraie & Geesink, 2006, Ouali *et al.*, 2006). Hence, measurement of meat using Raman spectroscopy at 5 d PM could provide a greater understanding of the biochemical processes which result in increased tenderness.

Consequently, six experiments over three years were conducted to investigate the potential for the hand held Raman spectroscopic device to predict the shear force values of fresh intact lamb muscles. Given the economic value of the *m. longissimus lumborum* (LL) to a carcase and the

external positioning of the *m. semimembranosus* (SM) making it ideal for online measurement, these two muscles were selected for investigation. An additional experiment (experiment 6) was conducted to determine the impact of freezing and thawing muscles on the prediction of shear force given the discrepancies between the previous research conducted by Schmidt *et al.* (2013) and the initial experiment conducted in this project.

3.1.2 Materials and methods

Samples

An initial experiment (Experiment 1) was conducted using samples of loin (Product identification number HAM 4866; Anonymous, 2005) and topside (Product identification number HAM 5077; Anonymous, 2005) which were collected from the same abattoir over four consecutive measuring days.

Further experiments (Experiments 2 – 6), were conducted using topside (Product identification number HAM 5077; Anonymous, 2005) collected from a second abattoir over a two-year period. Samples for each experiment were collected over four consecutive days. Samples to investigate the impact freezing and thawing (Experiment 6) were collected over two days (45 on day 1 and 35 on day 2) from the same abattoir. The total number of samples and the number of samples collected per day are outlined for each experiment in Table 1.

Table 1. The muscles samples, number of samples collected and samples collected per day for each experiment conducted to meet objective 1.

Experiment	Muscle Sampled	Number of Samples Collected	Samples Collected per day	Number of Days
1	*m. longissimus lumborum*[*]	80	20	4
	m. semimembranosus[*]	80	20	4
2	*m. semimembranosus*	80	20	4
3	*m. semimembranosus*	32	8	4
4	*m. semimembranosus*	32	8	4
5	*m. semimembranosus*	80	20	4
6	*m. semimembranosus*	80	45 & 35	2

[*]denotes samples collected from the same carcasses

All samples were randomly selected from different consignments and were of unknown background, sex and age, representing animals typically processed by the abattoir in order to obtain a spread in shear force values. All lambs were processed following commercial slaughter processes and while lamb carcasses in experiment 1 were not subjected to electrical stimulation, the lamb carcasses in experiments 2 – 6 were electrically stimulated with a mid-voltage unit (2000mA with variable voltage to maintain a constant current, for 25 s at 15 pulses/s, 500 microsecond pulse width, unipolar waveform) (Toohey *et al.*, 2008).

In each experiment at 24 h the samples were boned out from the carcasses. Once the topsides were boned out, the cap muscle (*m. gracilis*) and *m. adductor* were removed to leave the *m. semimembranosus* (SM) for measurement.

Raman Spectroscopy: Objective 1 - Longissimus Lumborum

At 24 h post slaughter, Raman spectroscopic measurements were conducted at ambient room temperature on the samples once they had been removed from the carcase. Prior to measurement, the Raman spectroscopic device was calibrated on polystyrene. Raman spectra were then collected on the chilled intact muscle with the silver skin removed (Figure 1) at ambient temperature using a hand held Raman spectroscopic device with a 671nm laser using 70mW of power.

Figure 1. Hand held Raman spectroscopic device showing the measurement of the *m. longissimus lumborum* with the epimysium removed.

The initial experiment was conducted with an integration time of 3 seconds for measurement with 1 accumulation. Twelve (12) Raman measurements of the muscle were taken along each of the caudal and medial portions of the LL, perpendicular to the muscle fibre direction 24 hour PM (Figure 1). Ageing treatments (24 hour and 5 days PM) were allocated across the caudal and medial portions of LL in a balanced manner across carcasses and the remaining cranial portion was removed and frozen at -20 ºC for IMF analysis (data reported in Objective 3). After Raman spectra were collected 24 hour PM, LL portions allocated to 5 days post slaughter ageing were vacuum packed and held at -1˚C for 4 days (data reported in Objective 2).

Semimembranosus

Raman spectroscopic measurements were conducted at ambient room temperature at 24 h PM on a fresh cut surface of the intact SM with the epimysium removed (Figure 2). Twelve positions were scanned using a Raman hand held device (Schmidt *et al.*, 2010) perpendicular to the muscle fibre, over the face where the *m. adductor* had been removed.

Figure 2. Hand held Raman spectroscopic device showing the measurement of the *m. semimembranosus* with the epimysium removed.

Spectra were recorded using 70mW of laser power and an integration time of 3.75 seconds and 1 accumulation for the initial investigation (experiment 1). To facilitate the comparison between different total measurement times during experiments 2-6, the first integration (total measurement 3 s) from each Raman spectroscopic measurement was saved separately to a scan which included 10 accumulations (total measurement 15 s) at the same position on the muscle.

After scanning with the Raman spectroscopic hand held device and removal of sections for the measurement of traditional indicators, the remaining SM samples were vacuum packed and held in chilled storage for four days.

Objective 2: Longissimus Lumborum

After Raman spectra were collected 24 h PM during the initial experiment, LL portions allocated to 5 days post slaughter ageing were vacuum packed and held at -1°C for 4 days. At 5 days PM, the vacuum packs were opened for 2 hours, allowing samples to 'bloom' so the metmyoglobin could re-bind to oxygen (Lee *et al.*, 2008) and a freshly cut (very fine surface removed) area was scanned to avoid losing the weak Raman signal due to fluorescence and saturation (McCreery, 2000). As with previous Raman spectroscopic measurements, scans at day 5 PM were also conducted perpendicular to the muscle fibre direction, with the same parameters used 24 h PM.

Semimembranosus

During experiments 2-5, after scanning with the Raman probe and removal of sections for measurement of traditional indicators, SM samples were vacuum packed and held at 1°C for 4 days. At 5 days PM, SM samples were removed from the vacuum packs and oxygenated ('bloomed') for 2 hours prior to rescanning a freshly cut surface using the same parameters described for 24 h PM Raman spectroscopic measurements.

Freeze/Thaw Experiment

Raman spectroscopic measurements were conducted 24 hours, 5 and 8 days PM. Raman spectroscopy measurements were taken 24 hours PM on the *m. semimembranosus* after it had been removed from the carcase and the subcutaneous fat and silverskin had been removed. A 671nm hand held Raman spectroscopic device was used to conduct 10 spectral measurements on each SM on a freshly cut surface perpendicular to the muscle fibre, at ambient room temperature. Spectra were recorded using 70mW of laser power and an integration time of 3 seconds and 5 accumulations (total measurement time 15 seconds). Once the 24 h PM Raman spectroscopic measurements were completed and sections for testing traditional indicators of tenderness had been excised, the remaining portion of SM was vacuum packed and held at 2.5°C for 4 days.

At 5 days PM, SMs were removed from the vacuum packs, allowed to oxygenate or 'bloom' for 2 hours and a freshly cut surface was re-measured with the Raman hand held device, using the same parameters described for 1 day PM. After Raman spectroscopic scans at 5 days and the sampling for traditional indicators had been completed, the remaining SM was vacuum packed and frozen at -20°C.

After being held frozen at -20 ºC for 24 hours, SMs were thawed for 21 hours at 0.6°C (8 days PM), and the samples were removed from the vacuum pack, allowed to bloom for 2 hours and a freshly cut surface was re-measured using the same spectral parameters as previously used for 24 h and 5 day PM Raman spectroscopic measurements.

Indicators of Tenderness

At 24 h PM once Raman spectra were collected, sections for measurement of traditional indicators measured at 24 h (Table 2) were excised to determine whether Raman spectra could provide a better prediction of meat quality compared to the traditional indicators. Once sections were removed, the remaining sample was vacuum packed and held for 4 days.

At 5 d PM, samples were removed from the vacuum pack and allowed to oxygenate ('bloom') for 2 h prior to Raman spectra being collected. Once 5 d Raman spectra were collected (data reported in Objective 2), further sections were excised to enable measurement of traditional indicators (Table 2).

After being frozen and thawed (8 days PM), SMs collected in experiment 6 were removed from vacuum packs, patted dry and weighed for freeze/thaw losses. Immediately prior to Raman spectroscopy measurements, SMs were allowed to bloom for 2 h and colour was measured again on a freshly cut surface. Once Raman spectra scans were completed, another 1 – 2 g section was removed for particle size (PS) measurement, a 25 g section for collagen determination and a 'block' prepared to measure shear force (mean 65 g).

Table 2. Indicators of tenderness measured, muscle sampled and time post mortem measurements were taken during each experiment.

Experiment	Muscle Sampled	Indicators Measured	Time Post Mortem
1	*m. longissimus lumborum*	shear force	24 h and 5 d
		cooking loss	24 h and 5 d
		particle size	24 h and 5 d
		pH_{24}	24 h
		pHu	5 d
		sarcomere length	24 h
		histology	24 h and 5 d
	m. semimembranosus	shear force	5 d
		cooking loss	5 d
		particle size	24 h and 5 d
		pH_{24}	24 h
		pHu	5 d
		sarcomere length	24 h
2	*m. semimembranosus*	shear force	5 d
		cooking loss	5 d
		particle size	24 h and 5 d
		pH_{PR}	1 h
		pH_{24}	24 h
		pHu	5 d
		sarcomere length	24 h
3	*m. semimembranosus*	shear force	5 d
		cooking loss	5 d
		particle size	24 h and 5 d
		pH_{PR}	1 h, 2 h, 3h and 4 h
		pH_{24}	24 h
		sarcomere length	24 h
4	*m. semimembranosus*	shear force	5 d
		cooking loss	5 d
		particle size	24 h and 5 d
		pH_{PR}	1 h, 2 h, 3h and 4 h
		pH_{24}	24 h
		sarcomere length	24 h
5	*m. semimembranosus*	shear force	5 d
		cooking loss	24 h and 5 d
		particle size	24 h and 5 d
		pH_{PR}	1 h
		pH_{24}	24 h
		pHu	5 d
		sarcomere length	24 h
		total collagen	5 d
		soluble collagen	5 d
6	*m. semimembranosus*	shear force	5 d
		cooking loss	24 h and 5 d
		particle size	24 h and 5 d
		pH_{PR}	1 h
		pH_{24}	24 h

pHu	5 d
sarcomere length	24 h
total collagen	5 d
soluble collagen	5 d

Shear force (SF) tests were conducted on blocks cut from the middle of the muscle and cooked at 71°C for 35 min. Measurement was completed using a Lloyd texture analyser with a vee-blade, as described by Hopkins *et al.* (2011a). SF measurements used were the mean of 6 replicate values, except where the co-efficient of variation exceeded 24% then the median value of the 6 replicates was used (Hopkins *et al.*, 2012). Blocks were weighed before and after cooking to determine cooking loss (CL).

The pH values pre–rigor (pH_{PR}) and at 24 h (pH_{24}) were determined using a TPS® Intermediate Junction pH electrode with a BNC plug calibrated using pH buffers (pH 4.0 and 6.0) held at ambient temperature. pHu values were determined using 2.5g of muscle homogenate in 10 ml of 5 mM iodoacetate/150 mM KCl (pH adjusted to 7.0), as explained by Dransfield *et al.* (1992).

Sarcomere length (SL) was measured using the laser diffraction method as previously described by Bouton *et al.* (1973) and particle size (PS) was determined using a 1-2 g section of muscle homogenised at 16 000 rpm, as previously described by Karumendu *et al.* (2009). Because the results of PS analysis are variable, a quality assurance method was used to ensure that the variation did not affect the statistical analysis (Hopkins *et al.*, 2014).

Sections excised for histological imaging were fixed in a solution of 2.5% glutaraldehyde and 2% paraformaldehyde in 0.1M phosphate buffer (adapted from Taylor & Frylinck (2003). Embedding and staining was completed before images were taken on a Leica DMR microscope and Nikon DXM 1200F digital camera, and total and partial breaks across the myofibril were quantified over 45 fibres per sample (Hopkins *et al.*, 2007).

Total collagen (TC) was determined using 0.1 g of freeze dried homogenised meat, hydrolysed in 3 ml of 3.5 M H_2SO_4, diluted with 3.75 ml water and 0.25 ml of 2 M NaOH, oxidised, heated at 60º C in a water bath for 15 min and cooled, before the absorbance of the solution was measured at 558nm, as described in the AOAC standard (AOAC, 2000). Soluble collagen (SC) was measured using 0.5 ml of filtered supernatant made of 1.5 g freeze dried meat in 10 ml of water, heated and mixed, with the insoluble material removed. This supernatant was hydrolysed in 3 ml of 3.5 M H_2SO_4 and measured as per total collagen (AOAC, 2000).

Data Analysis

On each day prior to RS measurements, the device was calibrated using polystyrene and a RS measurement without using the laser or 'dark scan' was completed to determine the background interference. This background was removed from the spectra before they were saved as raw data. Principal Component Analysis (PCA) was performed using MATLAB 7.9.0 (R2009b) software (TheMathWorks Inc., Natick, MA, USA) on muscle spectral data to identify spectra that didn't relate to meat and ascertain 'clean' meat spectral data without interference that were not detected and removed at measurement. Sub-sets of spectra for each sample were then averaged and the wavelength frequencies were reduced to a range of 500-1800cm^{-1}.

For the models from the initial experiment, the k-fold (k=8) cross validation method was used to determine the number of latent vectors to include. The number of latent vectors was chosen based on the number of components with the minimum average cross validated root mean square error of prediction (optimal RMSEP) across 20 replicates of the k-8 cross validation.

However, the most appropriate model to report from experiment 5 was determined using the Monte-Carlo cross validation method (Arlot & Celisse, 2010) with K = 8 and 50 random repeats. Unlike the k-fold method, the Monte-Carlo cross validation selected the optimal model by selecting the simplest model with the minimum cross validated average mean squared prediction error ($MSPE_{cv}$) subject to the one standard error rule (Hastie *et al.*, 2008). Using this rule, the "optimal" model selected is the most parsimonious model having average mean $MSPE_{cv}$ less than the average $MSPE_{cv}$ plus associated error for the model with minimum average mean $MSPE_{cv}$.

Once the number of latent vectors had been established, partial least squares regression analysis (PLS) was fitted using leave one out (LOO) cross validation to determine the correlation between the predicted shear force values based on the spectra and observed shear force values. A Null model of the observed shear force values was obtained by predicting the average shear force value leaving one observation out at a time. Further models combining Raman spectra and the traditional indicators of shear force were also fitted using PLS regression. Summaries for PLS models, where given, include the Root Mean Square Error of Prediction (RMSEP) or Square-root $MSPE_{cv}$ ($RMSPE_{cv}$) for the null and optimal models, relative reduction in the RMSEP or $RMSPE_{cv}$ (null and optimal model), and the squared correlation between the observed trait and the Leave-One-Out (LOO) cross validated predictions (R^2_{cv}). All calculations were conducted using R statistical software (R Core Team, 2013) using the *pls* package (Mevik *et al.*, 2011).

Models for the prediction of shear force based on traditional indicators including SL, pHu, CL, breaks across the myofibril and/or PS for experiment 1 were fitted using simple linear regression. Models to determine the relationship between shear force and traditional indicators for experiment 5 were fitted using simple linear regression, simplified using step wise regression (full data reported in attached published papers and thesis).

3.1.3 Results
Traditional Indicators

Summary statistics for the shear force values and traditional indicators measured in the 5 experiments are outlined in Table 3.

Table 3 Summary Statistics for the traditional indicators measured for each experiment.

Experiment	Muscle Sampled	Indicators Measured		Mean (S.D)	Range (min, max)
1	LL	shear force (N)	24 h	60 (13.7)	34.8 - 87.1
			5 d	38.8 (9.9)	20.9 - 64.6
		cooking loss (%)	24 h	17.3 (2.7)	11.3 - 25.9
			5 d	19.1 (4.3)	9.8- 28.8
		particle size (µm)	24 h	196 (66.6)	83 - 433
			5 d	127 (24.2)	84 - 236
		pH_{24}		5.69 (0.16)	5.54 - 6.29
		sarcomere length (µm)		1.65 (0.09)	1.36 - 1.86
		myofib. breaks (%)	24 h	0.13 (0.22)	0 - 1.4
			5 d	0.67 (0.57)	0 - 2.2
	SM	shear force (N)		51.4 (13.1)	29.2 - 78.4
		cooking loss (%)		19.2 (3.7)	0.2 - 28.8
		particle size (µm)	24 h	229 (46.8)	159 - 455
			5 d	166 (40.8)	95 - 322
		pHu		5.6 (0.1)	5.5 - 6.2
		sarcomere length (µm)		1.7 (0.03)	1.46 – 2.0
2	SM	shear force (N)		45.4 (9.4)	26.3- 74.3
		cooking loss (%)		22.2 (2.0)	15.5- 26.3
		particle size (µm)	24 h	266.9 (58.9)	134.3- 399.6
			5 d	166.4 (37.6)	104.8- 273.3
		pH	pH_{PR}	6.19 (0.21)	5.68- 6.8
			pH_{24}	5.59 (0.08)	5.47- 6.05
			pHu	5.52 (0.10)	5.4- 6.1
		sarcomere length (µm)		1.80 (0.11)	1.47- 2.06
3	SM	shear force (N)		40.0 (8.8)	24.9- 59.4
		cooking loss (%)		21.5 (2.2)	16.0- 26.0
		pH	pH_{PR}	1 h	6.14 (0.2)	5.79- 6.83
			2 h	5.78 (0.26)	5.10- 6.55

Group	Muscle	Measurement	Subtype	Time	Mean (SD)	Range
				3 h	5.65 (0.20)	5.43- 6.29
				4 h	5.65 (0.18)	5.45- 6.33
			pH_{24}		5.58 (0.12)	5.42- 6.05
		sarcomere length (µm)			1.85 (0.11)	1.61- 2.11
4	SM	shear force (N)			30.4 (7.5)	20.4- 49.8
		cooking loss (%)			21.0 (2.3)	15- 24.7
		pH	pH_{PR}	1 h	6.20 (0.3)	5.65- 6.87
				2 h	5.88 (0.28)	5.49- 6.6
				3 h	5.75 (0.26)	5.43- 6.25
				4 h	5.66 (0.15)	5.45- 6.11
			pH_{24}		5.65 (0.08)	5.50- 5.85
		sarcomere length (µm)			1.83 (1.52)	1.44- 2.30
5	SM	shear force (N)			40.2 (9.4)	24.7 - 76.8
		cooking loss (%)			23.9 (2.6)	14.8- 34.9
		particle size (µm)		24 h	254 (52.4)	128- 376
				5 d	182 (46.3)	83- 299
		pH	pH_{PR}		6.02 (0.20)	5.47 - 6.80
			pH_{24}		5.68 (0.15)	5.44 - 6.12
			pHu		5.71 (0.10)	5.59 - 6.16
		sarcomere length (µm)			1.59 (0.16)	1.26 -1.89
		collagen (mg/g)	total		13.1 (2.2)	9.1 - 22.3
			soluble		0.49 (0.08)	0.3 - 0.8
6	SM	shear force (N)			37.1 (7.7)	19.8 – 58.8
		cooking loss (%)			23.9 (2.6)	16.6 – 31.7
		particle size (µm)		24 h	254 (52.4)	131 – 388
				5 d	187 (52.5)	107 – 365

pH	pH_{PR}	6.02 (0.20)	5.47- 6.80
	pH_{24}	5.68 (0.15)	5.44- 6.12
	pHu	5.71 (0.10)	5.59- 6.16
sarcomere length (µm)		1.75 (0.19)	1.75 – 2.10
collagen (mg/g)	total	0.49 (0.08)	0.3 – 0.8
	soluble	13.1 (2.2)	9.1- 22.3

Objective 1

As illustrated in Table 4, prediction of the shear force values using Raman spectra collected at 24 h PM gave a limited ability to predict shear force values of the *m. semimembranosus* in the initial experiment (12.9% reduction in the prediction error, R^2_{cv} = 0.26; Fig 3). However, no other model indicated a potential to predict shear force. The prediction error and accuracies of models from experiments 2, 3 and 4 are not reported as failure of an electronic component within the probe resulted in poor quality spectra which were not able to be used for predictions.

Table 4. Model results for the prediction of shear force values at 5 days post mortem using Raman spectra collected at 24 h post mortem for the 6 experiments.

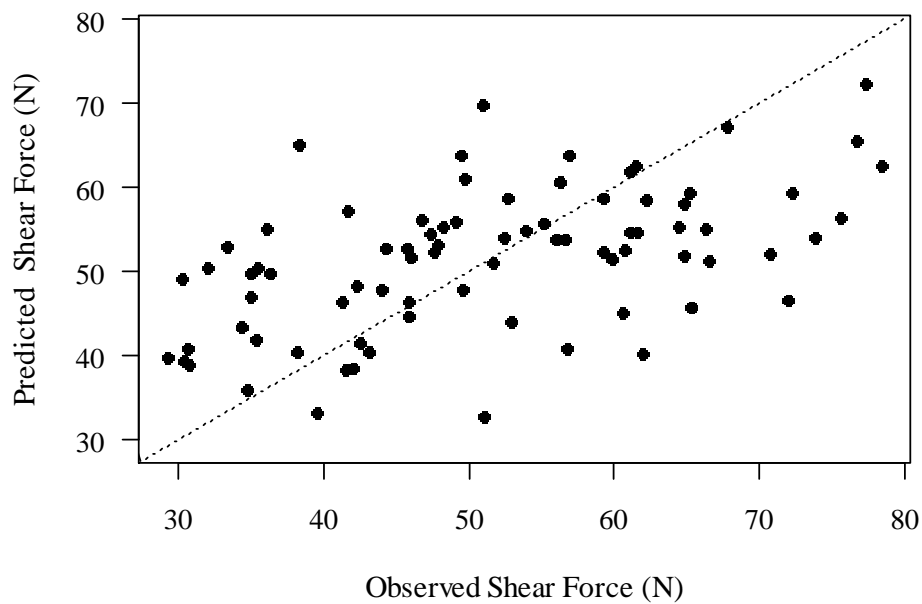| Experiment	Muscle	Root Mean Squared Error of Prediction		Reduction in Error (%)	R^2_{cv}
		Null	Optimal		
1	LL	10.0	10.0	0	0.00
	SM	13.2	11.5	12.9	0.26
2	SM	–	–	–	–
3	SM	–	–	–	–
4	SM	–	–	–	–
5	SM	9.4	9.4	0	0.00
6	SM	7.69	7.69	0	0.00

Figure 3. Cross validated prediction of SM shear force values (N) measured 5 days post mortem using Raman spectra taken 24 h post mortem (Experiment 1).

The prediction error of models from experiment 1 predicting shear force values of the SM indicated that using Raman spectra to predict shear force values yielded a more precise model than models using the traditional indicators (RMSEP = 11.5 and 13.9, respectively; Table 5).

Table 5. The error of prediction (RMSEP) for models using traditional indicators and/or Raman spectra collected at 24 h to predict shear force values (N) of lamb SM at 5 days post mortem.

Model Covariates	RMSEP (N)	Reduction in Error
Null	13.2	-
Cooking Loss (CL)	13.3	- 1.0
Sarcomere Length (SL)	13.2	0
pHu	13.8	- 4.5
CL, SL and pHu	13.9	- 5.3
Raman Spectra	11.5	12.9
Raman Spectra + CL, SL and pHu	12.0	9.1

In Table 6, the RMSEP values for the cross validated prediction models using the traditional indicators (sarcomere length, cooking loss and/or pHu) and Raman spectra collected 24 h PM to predict shear force values of the LL at 24 h and 5 days PM are summarised.

17

Table 6. The RMSEP for models using traditional indicators and Raman spectra collected at 24 h to predict shear force values (N) of lamb LL 24 h and 5 days post mortem.

Model Covariates	Shear Force (N)		Relative Reduction in RMSEP (%)	
	(24 h)	(5 Day)	(24 h)	(Day 5)
Null	14.0	10.0	—	—
Cooking loss (CL)	13.5	9.7	3.6	3
Sarcomere length (SL)	12.9	10.1	7.9	- 1.0
pH_{24}	14.0	10.1	0	- 1.0
PS	14.0	10.2	0	- 2.0
Myofibrillar breaks (MB)	13.8	9.8	1.4	2.0
CL, SL, PS, pH_{24} and MB (all available)	13.4	9.9	4.3	1.0
Raman Spectra	13.6	10.0	2.9	0
Raman Spectra + CL, SL, PS, MB and pH_{24}[+]	13.6	—	2.9	—
Raman Spectra + CL, SL, PS,MB and pH_{24}*	—	10.0	—	0

[+] Model 24 h data for LL portion allocated to 24 h PM ageing period.
*Model 24 h data for LL portion allocated to 5 day PM ageing period.

Of the indicators reported (Table 6) the most precise model for predicting shear force at 24 h used sarcomere length (RMSEP = 12.9), however although overall the relationship between shear force values and sarcomere length is weak (R^2= 0.14; Figure 4). There was small improvements in the precision of models that included the traditional indicators and Raman Spectra as covariates, although these improvements (RMSEP = 13.2 – 13.4) were marginal in comparison to the null model (RMSEP = 13.8).
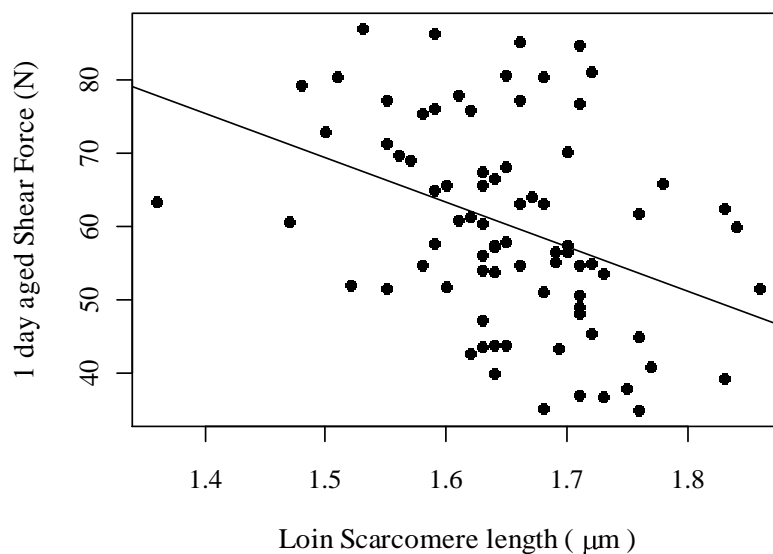
Figure 4. The relationship between LL shear force values (N) and sarcomere length (µm) 24 h PM.

Results from the chemometric analysis of data from Experiment 5 suggests that there is no improvement to the prediction of shear force values when the total measurement time is increased from 3 s to 15 s (Table 7). Furthermore, the accuracy and precision of the prediction of shear force using Raman spectra measured at 24 h was not improved when the samples were frozen and thawed after 5 days ageing prior to the measurement of shear force values.

Table 7. Summary chemometrics for the prediction of shear force values using Raman spectra measured 24 h post mortem using the first integration (3 s) and the full accumulation (15 s).

Optimal RMSEP$_{CV}$ (Latent Vectors)		Null RMSEP$_{cv}$
First Integration	**Full Accumulation**	
9.41 (0 LV)	9.43 (0 LV)	9.40

Objective 2

The results of the chemometric analysis suggest that there is a limited ability to predict shear force values using Raman spectra measured 5 d PM. While experiment 1 indicated there was some potential to predict shear force values of SM (7.6% reduction in prediction error, R^2_{cv} = 0.16), further experiments were unable to replicate this result.

Table 8. Model results for the prediction of shear force values at 5 days post mortem using Raman spectra collected at 5 d post mortem for the 5 experiments conducted.

Experiment	Muscle	Root Mean Squared Error of Prediction		Reduction in Error (%)	R^2_{cv}
		Null	Optimal		
1	LL	10.0	13.3	- 33.0	0.08
	SM	13.2	12.3	7.6	0.16
2	SM	–	–	–	–
3	SM	–	–	–	–
4	SM	–	–	–	–
5	SM	9.42	9.42	0	0.00
6	SM	7.69	7.69	0	0.00

Based on the RMSEP criterion, the prediction of shear force values of SM using Raman spectra measured at 5 days PM has a greater reduction in the prediction error (7.5%) compared to traditional indicators which showed an increase in the error of the prediction (- 5.3 – 0 %).

Table 9. The RMSEP for models using traditional indicators and/or Raman spectra collected at 5 days post mortem to predict shear force values (N) of lamb SM at 5 days post mortem.

Model Covariates	RMSEP (N)	Reduction in Error (%)
Null	13.2	
Cooking Loss (CL)	13.3	- 0.75
Sarcomere Length (SL)	13.2	0
pHu	13.8	- 4.5
CL, SL and pHu	13.9	- 5.3
Raman Spectra	12.2	7.5
Raman Spectra + CL, SL and pHu	13.0	- 1.5

The prediction error of the models to predict LL shear force at 5 days PM (Table 9) show that the most precise model is gained by using cooking loss (RMSEP = 9.7; Null RMSEP = 10.0). Although this is only marginally more precise than the combination of all three traditional indicators and Raman spectra collected 5 days post mortem (RMSEP = 9.8) or the percentage of myofibrillar breaks (RMSEP = 9.8).

Table 10. The RMSEP for models using traditional indicators and Raman spectra collected at 5 days post mortem to predict shear force values (N) of lamb LL at 5 days post mortem.

Model Covariates	Shear Force (N)	Relative Reduction in RMSEP (%)
Null	10.0	—
Cooking loss (CL)	9.7	3
Sarcomere length (SL)	10.1	- 1.0
pH_{24}	10.1	- 1.0
PS	10.2	- 2.0
Myofibrillar breaks (MB)	9.8	2.0
CL, SL, PS, pH_{24} and MB (all available)	9.9	1.0
Raman Spectra	10.0	0
Raman Spectra + CL, SL, PS, MB and pH_{24}	10.0	0

Models from experiment 6 indicate that freezing and thawing samples prior to measurement of shear force values after 5 days ageing did not improve the accuracy and error of the prediction using Raman spectra collected at 5 days PM. Furthermore, inclusion of any other indicator or combination of indicators as predictors in the model did not improve the prediction models.

3.1.4 Discussion

Prediction of Shear Force

Prediction models described in the results of both Objectives 1 and 2 indicate that the Raman spectroscopy hand held device is currently unable to provide robust and repeatable predictions of shear force in lamb. Throughout the experiments conducted, investigation into the potential use of the Raman hand held device was plagued by electronic issues. Consequently, poor quality spectral data were collected during experiments 2, 3 and 4 conducted in 2013 and further instabilities in the electronic components within the hand held device may have contributed to the poorer predictions found in experiments 5 and 6 conducted in 2014. These issues over the years have been the result of ageing electronic components in the device, the electronic components wearing due to the number of samples measured during consecutive experiments and a short in the electronics caused by the use of a faulty European to Australian conversion electrical plug. However, further development of the Raman spectroscopic hand held device, including updating the aging electronic components and conversion of the power source plug to an Australian plug should be able to overcome these instability issues.

The best R^2 between cross validated predictions and observed values (R^2_{cv}) was the prediction of shear force values for SMs at 5 days PM using the Raman spectra measured 24 h PM. Comparison of this model to the Raman study conducted on frozen and thawed lamb loin indicates that the prediction accuracy in this study is lower than previously reported, as Schmidt *et al.* (2013) reported R^2 coefficients of 0.72 and 0.86 when predicting shear force values on data sets collected from carcasses from 2 different sites. While both studies were conducted on intact lamb samples, it must

be stressed that there is a limited ability to compare between studies. Since sample handling varies greatly between the experiments conducted in this study and that of Schmidt *et al.* (2013) it was hypothesised that freezing and thawing of samples was responsible for the differences in predictions found. This was proposed because Raman is sensitive to the freezing and thawing of proteins (Li-Chan *et al.*, 1994, Herrero, 2008a) as changes to the biochemical characteristics of the muscle occur during the freezing and thawing of meat. This is a consequence of the movement of water out of cells and cellular membranes during freezing, resulting in an increase in solutes and a loss in extractability of the myofibrillar fraction (Sikorski, 1978). It was hypothesised that movement of water within the myofibril during freezing could remove some of the overlap effect of solvent water within Raman spectra improving the predictions.

However a further experiment (experiment 6) disproved this hypothesis. It is possible that the variation in predictability between studies is a result of the difference in spectral acquisition parameters. While the research presented here was conducted by collecting 10 Raman spectra measured perpendicular to the muscle fibre over the largest face of the SM where the *m. adductor* was removed, Schmidt *et al.* (2013) measured 3 cm blocks of loin that had been quartered before 5 different positions were measured on the freshly cut surfaces with integration times of 5 and 4 s for the two sample groups. Thus, Schmidt *et al.* (2013) collected 15 spectra per sample over a much smaller portion of muscle. Furthermore, other Raman spectroscopic studies on pork (Beattie *et al.*, 2008) and beef (Beattie *et al.*, 2004b) have used integration times of 6 minutes and 3 minutes which produced relatively high R^2_{cv} values of 0.77 and 0.75 (Beattie *et al.*, 2004b, Beattie *et al.*, 2008). Although experiments in this project indicated that increasing the total integration time from 3 s to 15 s by increasing the number of 3 s accumulations from 1 to 3 did not improve prediction outcomes, the quality of the spectra was improved as the signal to noise ratio (SNR) was increased. This suggests that much longer integration times on considerably smaller portions of the muscle may be required to achieve the correlations coefficients previously reported. While a longer measurement time of 3 or 6 minute total measurement time would provide a substantial amount of quality Raman spectra, it is not a suitable approach for online measurement, and this does present a restraint with the adoption of current Raman technology.

Additionally, comparing the current Raman spectroscopic research with previous studies highlights that there are numerous experimental design factors which vary between studies, including the number of independent samples, the muscle and muscle face measured, positioning of the sample under the laser, the Raman spectroscopic device and wavelengths used as well as the methods of chemometric analysis, such as the pre-processing methods applied. For example, multiple studies previously conducted all aimed to predict shear force values determined by a Warner- Bratzler texture analyser using Raman spectra. However, as the experimental design of these studies cited vary greatly, it is difficult to determine the reasons for variation between findings. Consequently, further research is required to identify the optimal experimental design for measurement.

Of these, the number of positions and locations measured on each independent sample is critical as it determines the way in which the scattered light can be detected and the chemometric data can be analysed. Despite the widespread use of Principal Component Analysis as a tool for spectral data analysis, when PCA is used in the analysis of data from a small number of samples the average spectra representing each sample may under represent subtle differences between spectral regions of the samples (Bonnier & Byrne, 2012). This occurs because PCA clusters data based on spectral similarity and spatial distributions. Consequently, it is expected that Raman spectra

obtained from numerous sub-sections removed from a small number of independent samples would substantially impact on the variance and loadings which differentiate groups in further data analysis. This is because the strength of this analysis technique is in the loadings given that represent the spectral origin of the variations (Bonnier & Byrne, 2012). Such data sets with few truly independent samples are at risk of artificially biasing the results from chemometric analysis and consequently under representing subtle differences within more complex data sets. The models generated may then have a better accuracy of prediction than if the true spectral differences were represented. Consequently, better predictions are expected from studies such as Beattie *et al.* (2004b) who measured 168 pork LL sections from only 18 pigs. While the full impact is unknown as the models presented have not been tested on independent data sets, the low predictability of tenderness reported **does not** warrant further validation using the current hand held device and experimental parameters.

It is interesting to note that the prediction of shear force values using Raman spectra collected at 24 h post mortem yielded a better prediction than that using Raman spectra collected at 5 days. It is hypothesised that changes to the myofibrillar structure weakens the Raman signal when spectra are measured at 5 days PM. If changes to ionic strength during ageing are affecting the ability of Raman to predict shear force values, it is hypothesised that collecting spectra as the muscle enters *rigor* would improve the prediction, as ionic strength of sarcoplasmic fluid rapidly rises as the muscle enters *rigor* (Ouali, 1992).

Traditional Indicators

A comparison of shear force prediction models using both Raman spectroscopy and traditional indicators suggests that Raman spectroscopy yielded a more precise prediction than the prediction using the traditional indicators in experiment 2. Furthermore, using these traditional indicators of shear force for the SM it was found that none were significant in explaining the variation in shear force values ($P > 0.05$). Yet the ranges of traditional indicators found in this study represent those which would be expected from commercial flocks in Australia (Hopkins & Fogarty, 1998, Hopkins *et al.*, 2013).

Although, many previous studies have reported coefficients of determination (R^2) to describe the significance and the relationships between traditional indicators and shear force (Bouton *et al.*, 1973, Hood & Tarrant, 1981, Smulders *et al.*, 1990, Hopkins *et al.*, 2007), it needs to be recognised that linear relationships are dependent on the range of the data set. Consequently, they may not be a good measure of the merit of the calibration between data sets that have different ranges (Davies & Fearn, 2006). While previously cited studies are informative about the impact on shear force of extreme values of these indicators, these studies may not be reflective of the ranges that would be expected normally and as a result R^2 values reported by literature may not be accurate estimates of the differences which would be found in standard carcasses commonly processed (Davies & Fearn, 2006). Therefore, it is problematic to compare between studies that have used different experimental treatments and designs to highlight the interrelationships between shear force and the traditional predictors. For example, Bouton *et al.* (1971) influenced the pH to gain a wider range of values (5.6 – 7.0), whilst others have measured pH in different muscles (Karumendu *et al.*, 2009, Geesink *et al.*, 2011) and species (Smulders *et al.*, 1990, Scheffler *et al.*, 2013).

Furthermore, relationships between traditional indicators of tenderness, such as pH or sarcomere length and shear force values aren't always linear and may be confounded by other factors. This is highlighted by Hopkins *et al.* (2006) who found different processing conditions, such as electrical

stimulation and ageing, can constrain shear force values which then allows the full impact of other factors, such as age, nutrition and breed, on eating quality measurements to be established. Given that these relationships are not clear, it is not surprising that while the variation in shear force values explained by traditional indicators in this research varies between experiments, the findings presented here agree with some studies, but not with others.

The impact of processing techniques on the relationship between shear force and traditional indicators may also be responsible for variation in the prediction outcomes of different experiments. While experiment 5 and experiment 1 were conducted on fresh intact muscle using similar methodologies and sample handling, carcasses sampled in the experiment 1 were not subjected to electrical stimulation while carcasses sampled in experiment 5 were. Although reported improvements in tenderness have been inconsistent it has been found that electrical stimulation alters the rate of pH decline as treatment with electrical stimulation results in a temperature dependent acceleration of glycolysis following an immediate fall in pH value (Hwang *et al.*, 2003). While this doesn't alter the extent of glycolysis and pHu, it may remove the confounding effects of processing conditions on metabolic related traits. Consequently, breed, age and nutrition are responsible for more variation in shear force (Hopkins *et al.*, 2006) which is not accounted for in the present models since the samples were of unknown background in order to obtain a spread in shear force values and represent animals typically processed in commercial abattoirs.

The removal of confounding factors associated with background and age, may also explain differences in the prediction of shear force values using Raman spectra. While this study used samples collected from carcasses of unknown background, Schmidt *et al.* (2013) used samples collected from carcasses of first and second cross lambs in the sheep CRC nucleus flock at two different research stations that were slaughtered in two separate groups at 5 – 6 months of age. After completing the chemometric analysis jointly and separately for each group, Schmidt *et al.* (2013) noted coefficients of determination for prediction models were increased when two models were created based on site of origin. Consequently, the prediction of shear force values using Raman spectroscopy may be more accurate for the prediction of meat quality traits within lots which are of similar age and background.

3.1.5 Conclusion
Despite the initial experiment suggesting there was a limited ability to predict shear force values of fresh intact lamb, this finding was unable to be repeated in further experiments. Furthermore, inconsistent results were also found for the prediction of shear force values of intact lamb which had been frozen and thawed. Given these experiments were conducted over multiple years, it is likely that measurement with a Raman spectroscopic hand held device at either 1 or 5 days post mortem is unable to provide a robust and accurate prediction of instrumental measures of tenderness in lamb.

3.2 Objective 3
Establish what biochemical and biophysical changes the probe is detecting in relation to tenderisation and to explore the potential of the probe to provide measures of other traits such as fatty acids and intramuscular fat.

3.2.1 Introduction

In recent years there has been an increased focus on the management of meat quality of prime lambs in Australia, due to advances in meat grading systems for sheep meat products (Thompson *et al.*, 2005a). However, as lamb carcasses are assessed for market suitability using only weight, age, sex and fat scores, better carcase assessment tools are required by industry to determine whether lamb carcasses meet the quantitative and qualitative attributes vital to meeting the needs of domestic and export markets. Although there are numerous technologies which have been developed to assess carcase quality (Damez & Clerjon, 2008) few of these methods are suitable for measurement in commercial situations as they are destructive, time and labour intensive, require extensive sample preparation or bulky equipment. Recent advances in digital camera and laser technologies has facilitated greater research into optic methods as it has become possible to develop fibre optic components and energy efficient lasers suited for portable devices (Damez & Clerjon, 2008).

Raman spectroscopy (RS) is one such optic technology as it based on the inelastic scattering of light which provides information on the chemical composition of matter (Das & Agrawal, 2011). Therefore RS is a non-destructive tool which is potentially suitable for online measurement (Damez & Clerjon, 2008), consequently recent meat science studies have focused on it's potential to measure meat quality traits (Beattie *et al.*, 2008, Bauer *et al.*, 2013, Schmidt *et al.*, 2013).

Despite such studies indicating Raman spectra is capable of measuring other meat quality traits including pHu (R^2 = 0.94) (Scheier & Schmidt, 2013) and water holding capacity (r = 0.79) (Pedersen *et al.*, 2003) of fresh intact pork, previous RS studies on lamb have focused on the prediction of shear force values (Schmidt *et al.*, 2013, Fowler *et al.*, 2014a, Fowler *et al.*, 2014b). Consequently the potential to use RS to predict other indicators of meat quality of lamb has not been determined.

Furthermore, the potential to predict the level of intramuscular fat (IMF) and the major FA composition groups of lamb has not yet been established using the hand held Raman device even though bench top devices have demonstrated the ability to predict the species of origin of subcutaneous fat (Beattie *et al.*, 2007), measure and predict the fatty acid content and iodine value of pork adipose tissue (Olsen *et al.*, 2007, Olsen *et al.*, 2010, Lyndgaard *et al.*, 2011), determine whether pork has been affected by warmed over flavour (Brøndum *et al.*, 2000) and analyse fatty acid methyl esters (Beattie *et al.*, 2004a).

Therefore, a further two components were included in experiments 2 and 5 to evaluate the potential to predict pH, purge and colour as well as IMF level and the major FA group composition of fresh intact lamb using the hand held Raman spectroscopy device.

3.2.2 Prediction of other meat quality traits – Purge, colour and pH

Methods and Materials: Samples
As previously described for experiment 5 in Objectives 1 and 2, 80 lamb carcasses were measured over four consecutive days (20 per day) from the same abattoir. Carcasses were randomly selected from different consignments and were of unknown backgrounds, sex and age, representing animals that were typically processed at the abattoir in order to obtain a spread in shear force values. Lambs were processed following standard commercial slaughter processes and were electrically

stimulated pre-dressing with a mid- voltage unit (2000mA with variable voltage to maintain a constant current, for 25 s at 15 pulses/s, 500 microsecond pulse width, unipolar waveform) (Toohey *et al.*, 2008).

At 25 min post slaughter hot carcase weight (HCW) was recorded. Approximately 4 hours post slaughter GR tissue depth (depth of the tissue over the 12th rib, 110 mm from the midline) using a GR knife.

At 24 h post slaughter, topsides (Product identification HAM 5077; Anonymous, 2005) were removed (boned out) from the carcasses. The cap muscle (*m. gracilis*) and *m. adductor* were removed to leave the *m. semimembranosus* (SM) which was the muscle of measurement.

Raman Spectroscopy

Raman spectroscopic measurements were conducted prior to the onset of *rigor mortis* (pre- *rigor*) and at 24 h and 5 days post mortem.

Pre-rigor measurements were conducted 25 m PM on the SM *in-situ* with the subcutaneous fat and silverskin (epimysium) removed (Figure 5). Under abattoir conditions at an ambient temperature of 2°C, 10 positions were measured perpendicular to the muscle fibre. All measurements were taken with a 671 nm hand held Raman spectroscopic device (Schmidt *et al.*, 2013) and spectra were recorded using 70 mW of laser power and an integration time of 2 s. After measurement, the carcasses were chilled at a mean temperature of 3°C for 24 h.

Figure 5. Pre-rigor measurement of the *m. semimembranosus in-situ* in processing plant conditions.

At 24 h and 5 days post slaughter, Raman spectroscopic measurements were conducted at ambient room temperature on the SM once it had been removed from the carcase as previously described for experiment 5 in Objectives 1 and 2.

Traditional Indicators

Immediately prior to pre-rigor Raman spectroscopic measurements at 25 m PM, pH (pH_{PR}) and temperature ($temp_{20}$) of the SM was measured *in-situ* using a TPS intermediate junction pH electrode with a BNC plug calibrated using buffers (pH 4.01 and pH 6.86) held at ambient temperature.

At 24 h post mortem prior to measurement using the Raman device, a fresh cut was made on the muscle face where the *m. adductor* had been removed, the pH was re-measured with the pH electrode and a colour reading taken. Colour readings were taken using a Minolta® CR- 400 Colorimeter (Minolta Camera Co., Japan) under a D65 illuminant with an 8 mm aperture size, 10 degree observation angle and a closed cone that was calibrated using a white tile (Y = 92.8, X = 0.3160, Y = 0.3323).

At 5 days post mortem SMs were removed from vacuum packaging, patted dry with paper towel and weighed to determine purge. SMs were then allowed to 'bloom' for two hours before a finely cut surface was prepared on the same face previously measured and another colour reading was taken immediately prior to the Raman Spectroscopic measurement.

Data Analysis

Raw spectra were prepared for chemometric analysis as previously described in Objectives 1 and 2 (3.1.2). Sub-sets of spectra for each sample were averaged and wavenumbers reduced to a range of 500 – 1900cm^{-1}. Once the wavenumber was reduced, spectra were not subjected to alternative pre-processing techniques as previous studies have demonstrated that there was no significant improvement to the prediction outcomes when pre-processing was applied. Models to predict all meat quality indicators measured were then completed as outlined in section 3.2.1.

Models to determine relationships between pHu and traditional indicators were fitted using simple linear regression and simplified using stepwise regression.

Results

Summary statistics for HCW, GR depth, shear force, cooking loss, purge, pH, particle size analysis and colour are given in Table 10.

Table 11. Mean, standard deviation (SD) and range for carcase and eating quality indicators measured in Experiment 5.

Trait		Mean	SD	Range (min, max)
HCW (kg)		22.7	2.0	16.9 – 28.9
GR Fat (mm)		15	3.9	4 – 26
Shear Force (N)		40.2	9.4	24.7 – 76.8
Cooking Loss (%)		23.9	2.6	14.8 – 34.9
Purge (%)		2.7	1.2	1.1 – 6.4
pH	pH_{PR}	6.02	0.20	5.47 – 6.80
	pH_{24}	5.68	0.15	5.44 – 6.12
	pHu	5.71	0.10	5.59 – 6.16
Temp @ 25 m PM (ºC)		36.3	1.1	33.5 – 38.7
Sarcomere Length (µm)		1.59	0.16	1.26 – 1.89
Particle Size (µm) 24 h		254	52.4	128 – 376

	5 day	182	46.3	83 – 299
	$L*$	39.9	2.23	36.2 – 47.7
Colour 24 h PM	$a*$	16.0	1.39	12.6 – 19.3
	$b*$	-1.2	1.31	-3.3 – 3.3
	$L*$	38.3	2.12	33.8 – 44.2
Colour 5 day PM	$a*$	16.9	1.26	14.1 – 19.5
	$b*$	-0.3	1.12	-2.8 – 3.6
Collagen (mg/g)	soluble	13.1	2.2	9.1 – 22.3
	total	0.49	0.08	0.3 – 0.8

As highlighted by Table 12, spectra at 25 min post mortem were able to predict purge (reduction of $RMSEP_{cv}$ = 16.5%, R^2_{cv} = 0.32; Fig 6), (lightness) $L*$ (reduction of $RMSEP_{cv}$ = 12.0%, R^2_{cv} = 0.27) and pH_{24} (reduction of $RMSEP_{cv}$ = 6.6%, R^2_{cv} = 0.26). However, further models for the prediction of shear force demonstrated that Raman spectra measured at 25 min post mortem gave no ability to predict shear force values measured at 5 days post mortem.

Table 12. Chemometric analysis using Raman spectra measured 25m post mortem to predict meat quality indicators.

Indicator	Null Model $RMSEP_{cv}$	Optimal $RMSEP_{cv}$ (Latent Variables)	Relative Reduction $RMSEP_{cv}$ (%)	R^2_{cv}
Shear Force	9.42	9.42 (0 LV)	0	0.00
pH_{PR}	0.205	0.205 (0 LV)	0	0.00
pH_{24}	0.15	0.14 (6 LV)	6.6	**0.26**
pHu	0.10	0.10 (0 LV)	0	0.00
Sarcomere Length	0.16	0.16 (0 LV)	0	0.00
24 h PS	52.69	52.69 (0 LV)	0	0.00
5 Day PS	46.60	46.60 (0 LV)	0	0.00
Purge	1.15	0.96 (6 LV)	16.5	**0.32**
Total Collagen	2.25	2.25 (0 LV)	0	0.00
Soluble Collagen	0.08	0.08 (0 LV)	0	0.00
Cooking Loss	2.64	2.64 (0 LV)	0	0.00
24 h $L*$	2.25	1.98 (7 LV)	12.0	**0.27**
24 h $a*$	1.40	1.40 (0 LV)	0	0.00
24 h $b*$	1.32	1.26 (2 LV)	4.5	0.08

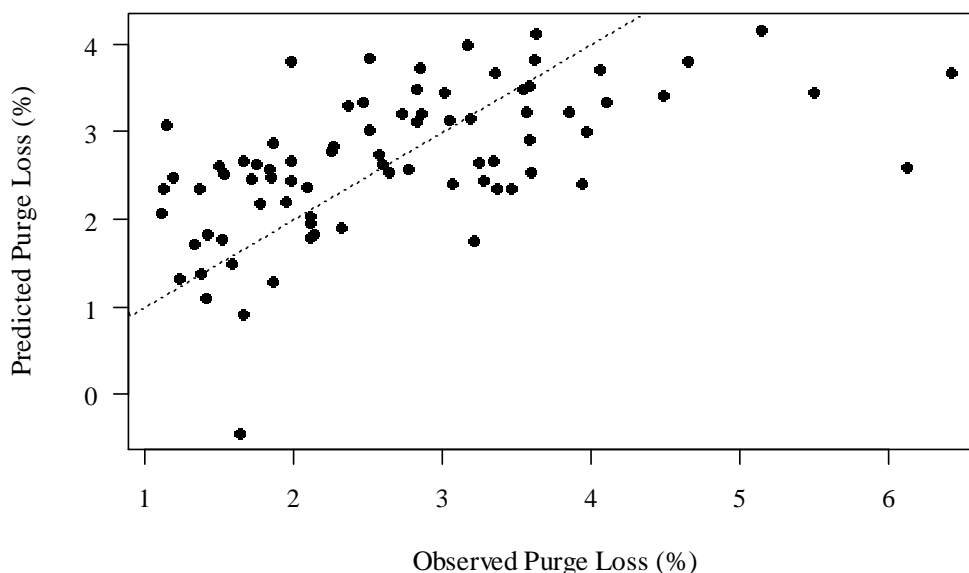|				
5 day *L**	2.13	2.13 (0 LV)	0	0.00
5 day *a**	1.27	1.27 (0 LV)	0	0.00
5 day *b**	1.13	1.13 (0 LV)	0	0.00

Figure 6. The cross validated correlation between purge (%) values predicted using Raman spectra and observed values measured from ovine *m. semimembranosus* after 4 days ageing.

As evident in Table 13, the predictions of pH_{24} and pHu using Raman spectra measured 24 h PM were improved in comparison to Raman spectra measured pre-rigor as shown in Table 11. The prediction of pH_{24} using Raman spectra measured 24 h PM gave a 20% reduction in $RMSPE_{cv}$ while the prediction for pHu gave a 30% reduction. The squared correlations between cross validated predicted values using Raman spectra and observed values were 0.48 and 0.59 (Fig. 7), respectively. There was also a greater ability to predict purge using Raman spectra measured 24 h PM (21.7% reduction in $RMSPE_{cv}$, R^2_{cv} = 0.42).

Table 13. Chemometric analysis using Raman spectra measured at 24 hours PM to predict indicators of meat quality.

Trait	Null Model RMSEP$_{cv}$	Optimal RMSEP$_{cv}$ (Latent Variables)	Relative Reduction RMSEP$_{cv}$ (%)	R^2_{cv}
pH$_{24}$	0.15	0.12 (8 LV)	20.0	**0.48**
pHu	0.10	0.07 (7 LV)	30.0	**0.59**
Sarcomere Length	0.16	0.16 (0 LV)	0	0.00
24 h PS	52.77	52.77 (0 LV)	0	0.00
5 Day PS	46.58	46.58 (0 LV)	0	0.00
Purge	1.15	0.90 (7 LV)	21.7	**0.42**
Cooking Loss	2.64	2.64 (0 LV)	0	0.00
Total Collagen	2.25	2.25 (0 LV)	0	0.00
Soluble Collagen	0.08	0.08 (0 LV)	0	0.00
24 h $L*$	2.45	1.96 (8 LV)	20.0	**0.32**
24 h $a*$	1.41	1.41 (0 LV)	0	0.00
24 h $b*$	1.32	1.32 (0 LV)	0	0.00
5 day $L*$	2.13	1.87 (1 LV)	12.2	0.22
5 day $a*$	1.27	1.27 (0 LV)	0	0.00
5 day $b*$	1.12	1.12 (0 LV)	0	0.00
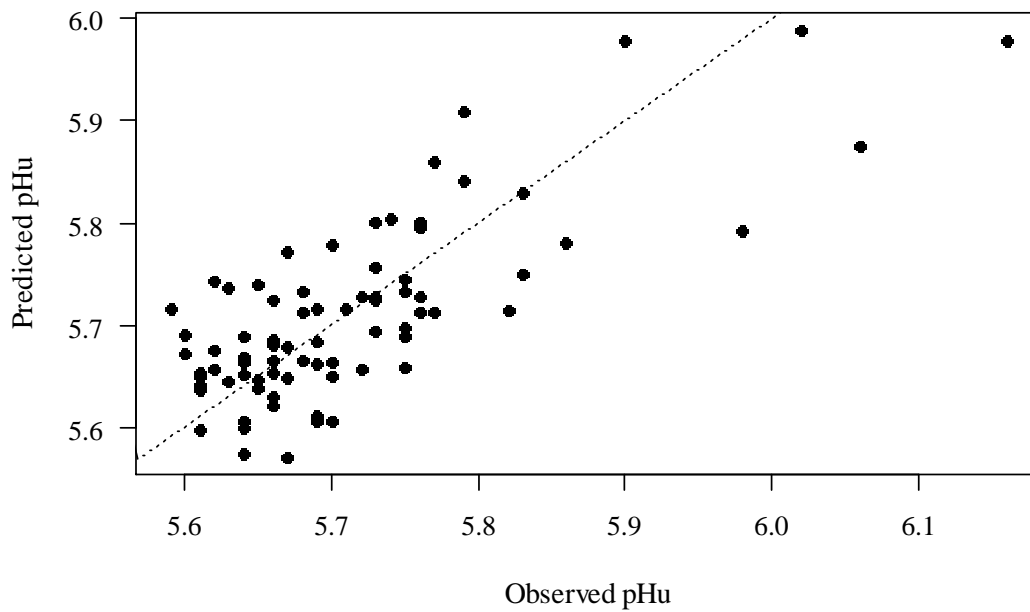
Figure 7. The cross validated correlation between pHu values of ovine _m. semimembranosus_ predicted using Raman spectra collected 24 h post mortem and measured at 5 days post mortem.

Using Raman spectra measured 5 days post mortem (Table 13) there was potential to predict only purge (18.3% reduction in $RMSPE_{cv}$, R^2_{cv} = 0.33; Fig 8).

Table 14. Chemometric analysis using Raman spectra measured at 5 days PM to predict indicators of meat quality.

Trait	Null Model RMSEP$_{cv}$	Optimal RMSEP$_{cv}$ (Latent Variables)	Relative Reduction RMSEP$_{cv}$	R^2_{cv}
pHu	0.10	0.10 (0 LV)	0	0.00
Sarcomere Length	0.12	0.12 (0 LV)	0	0.00
5 Day PS	46.57	46.57 (0 LV)	0	0.00
Purge	1.15	0.94 (6 LV)	18.3	**0.33**
Cooking Loss	2.64	2.64 (0 LV)	0	0.00
Total Collagen	2.26	2.26 (0 LV)	0	0.00
Soluble Collagen	0.08	0.08 (0 LV)	0	0.00
5 day $L*$	2.13	2.13 (0 LV)	0	0.00
5 day $a*$	1.28	1.28 (0 LV)	0	0.00
5 day $b*$	1.13	1.13 (0 LV)	0	0.00
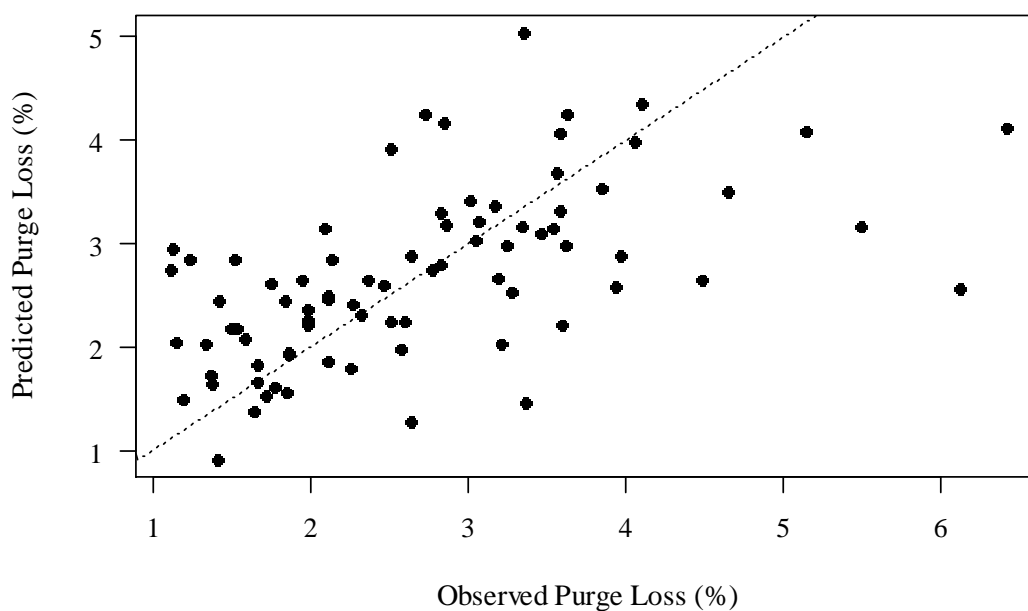
Figure 8. The cross validated correlation between predicted purge values (%) using Raman spectra collected 5 days post mortem and observed values of ovine *m. semimembranosus* measured after 4 days ageing.

32

It is also interesting to note that there is also potential to predict some colour parameters measured at 24 h and 5 days PM, such as $L*$ measured 24 h PM using Raman spectra measured pre rigor (12.0% reduction in $RMSPE_{cv}$, R^2_{cv} = 0.27; Table 12) and Raman spectra measured 24 h PM (20% reduction in $RMSPE_{cv}$, R^2_{cv} = 0.32; Table 13) as well as $L*$ measured at 5 days PM using Raman spectra measured 24 h PM (12.2% reduction in $RMSPE_{cv}$, R^2_{cv} = 0.22).

Using HCW, GR depth, $Temp_{pr}$, pH_{pr} and pH_{24} in a step-wise regression to determine the impact of meat quality indicators on pHu values demonstrated that of the indicators measured, pH_{24} is the only significant trait in determining pHu (R^2 = 0.27, P <0.001; Fig 9).
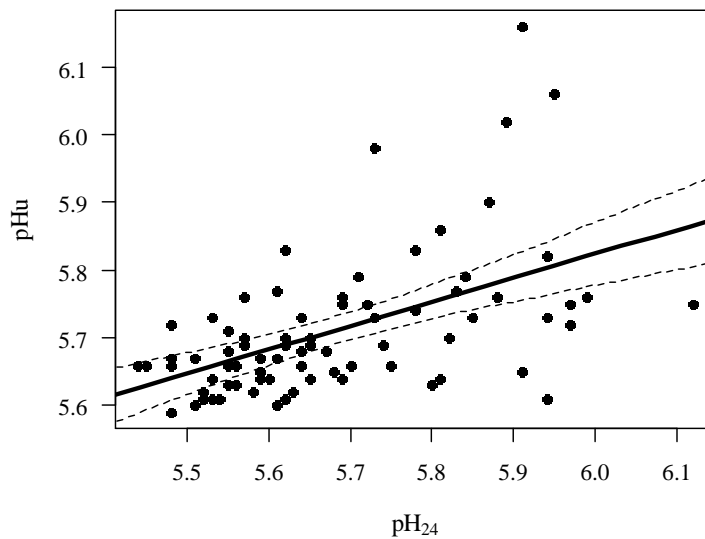
Figure 9. The correlation between observed pH_{24} and pHu values determined using a step-wise regression model (R^2 = 0.27, P <0.001).

As illustrated by Figure 10, declining pHu values are related to significant increases with purge (P = 0.004). The coefficient of the regression model indicates that for each unit increase in pHu value, purge decreases by – 0.029% (± 0.01).
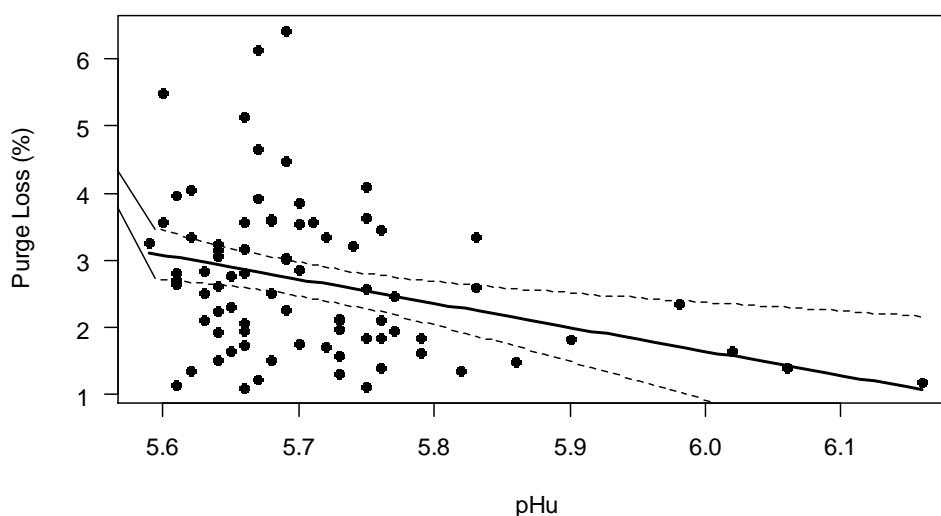

Figure 10. The relationship between observed pHu values and purge (%) of ovine *m. semimembranosus* measured at 5 day post mortem (R^2 = 0.10).

Discussion

Results of this study indicate for the first time that there is potential to predict pHu, pH_{24}, lightness (L^*), and purge of intact lamb SM using Raman Spectroscopy. While early post mortem measurements of Raman spectroscopy indicated that there is an ability to predict pH_{24} and purge, the most variation in these traits was described by spectra measured at 24 h post mortem. Given the relationships between pH, purge and colour and early post mortem metabolic events, it is plausible that Raman spectroscopy is only able to predict traits which are affected by metabolic processes or via metabolic substrates which are involved in the biochemical changes during the conversion of muscle to meat. Since spectra measured pre-rigor change rapidly due to continuing cell metabolism, metabolites may only be temporarily detectable (Scheier *et al.*, 2014). As a result it is possible that a single time pre-rigor measurement at 25 minutes post mortem is unable to provide enough information on the metabolic status of the muscle to be informative on the progression of rigor and subsequent meat quality indicators. Consequently, further investigation into the changes of spectra in lamb SM throughout the progression of rigor may provide a more optimal time post mortem to measure pre-rigor spectra facilitating the earlier identification of carcasses which are susceptible to quality issues as a result of deviating metabolic processes. This could be of particular relevance to the "heat toughening" condition observed in beef carcasses (Hopkins *et al.,* 2014).

Of the prediction models using spectra collected 24 h post mortem, the prediction of pHu and pH_{24} were the best models yielding cross-validated correlations between observed and predicted values (R^2_{cv}) of 0.59 and 0.48, respectively and reductions in prediction error of up to 30% when using Raman spectra for the prediction. The reduction in prediction of pH values at 24 h and 5 days using Raman spectra measured 24 h post mortem is unsurprising given that SMs with lower pH_{24} values tended to have lower pHu values. However, the prediction of pHu using Raman spectra collected at 24 h post mortem was more useful than using pH_{24} measured with the pH probe at 24 h.

As this is the first study to report the prediction of pH values in fresh intact lamb there is no existing literature to compare results, but previous studies have demonstrated the ability of Raman Spectroscopy to determine deviations in the pH decline of pork during the development of PSE like qualities (Scheier & Schmidt, 2013, Scheier *et al.*, 2014). This was possible as Raman signals which reflected inosine monophosphate (IMP), lactate, glucose 6-phosphate, PCr, phosphoric acid and ATP concentrations present in samples changed during the progression into rigor. Hence, collecting lactate and pH reference values of measured porcine SMs and synthesising reference spectra of metabolites, these studies were able to qualitatively define the biochemical changes that occur during the pH decline to the on-set of rigor. Although they indicate the Raman signals which would be expected to change with the on-set of rigor and describe the correlations that were found, a small number of carcasses (9 and 10 respectively) were sampled at increasing intervals from 0.5 h post mortem, which limits the application of findings to the quantitative prediction of pHu in lamb using Raman spectra measured 24 h PM.

While the prediction of pH_{24} and pHu are the best models using spectra collected at 24 h, it is interesting that models also demonstrated some ability to predict purge. Given that there is a significant relationship between purge and pHu values, it is plausible Raman spectroscopy is predicting purge indirectly through effects of pH on metabolic processes or via metabolic substrates which are involved in the biochemical changes during the conversion of muscle to meat that determine the meat's biophysical characteristics including pH. However, pHu prediction of

purge using Raman spectra measured 25 min or at 24 h PM gave lower prediction errors than prediction of purge using only the pHu values measured.

The review on the mechanisms of water holding capacity by Huff Lonergan & Lonergan (2005) further supports this hypothesis, stating the links between the early post mortem events particularly the rate and extent of pH decline, are critical in determining the ability of meat to retain moisture. Indeed, a study conducted by Pedersen *et al.* (2003) demonstrated that Raman microscopy was able to predict variation in drip loss of pork *m. longissimus dorsi* (0.83% prediction error, *r* = 0.95, 3 LV) during the first 45 min post mortem. Pedersen *et al.* (2003) proposed that this finding was consistent with the relationship between water holding capacity, pH, glycogen and protein conformation as changes to the NH stretching regions (3140 cm^{-1}) and α-helical band (940 cm^{-1}) were evident in spectra. However, as with previous Raman spectroscopic studies of pH decline because the focus is on pork the transference of these findings to the current study is limited.

Pork muscles are characterised by a greater concentration of type IIB muscle fibres in comparison to lamb and beef. These type IIB muscle fibres are white, fast twitch fibres which are easily fatigued (Kerth, 2013) due to the cell metabolism, oxidative capacity, contraction speed, fibre size, ATPase activity, myoglobin and glycogen content. Overall this increases glycolytic potential (Choe *et al.*, 2008, Choe & Kim, 2014), which is responsible for creating a faster rate of pH decline (te Pas *et al.*, 2004). Consequently, the pH decline of pork carcasses is usually completed in 6 – 12 hours PM with the on-set of rigor occurring at 4 – 6 hours PM (Savell *et al.*, 2005) depending on chiller regime and fat thickness (Huff Lonergan *et al.*, 2010). Hence, pork carcasses are more susceptible to meat quality issues, such as pale soft and exudative (PSE) meat, as a result of higher temperatures at rigor and increased rates of pH decline in the first 15 – 30 minutes post mortem (Savell *et al.*, 2005).

Increased purge and drip losses are associated with pH decline related quality issues, as evident in the study conducted by Melody *et al.* (2004) that found PSE affected carcasses had up to 10% of weight lost due to high purge. Since lamb carcasses undergo a slower rate of pH decline (te Pas *et al.*, 2004) and are smaller carcasses which consequently chill faster these same quality issues are not present. Therefore in comparison to lamb, deviations in water holding capacity and drip losses of pork may be more related to accelerated pH decline or on-set of rigor at earlier times post mortem and therefore at higher temperatures, which can be detected by the metabolic state determined by Raman spectroscopy (Pedersen *et al.*, 2003, Scheier *et al.*, 2014).

Yet it is also important to acknowledge the differences between pH decline and pHu as while accelerated pH decline can cause higher purge, the ultimate pH of muscles with accelerated pH declines may not be below normal ranges (Hwang *et al.*, 2004, Huff Lonergan & Lonergan, 2005). This is because pHu is a measure of the extent of pH decline and glycogen concentration of the muscle at slaughter (Choe & Kim, 2014) while pH decline is determined by cellular metabolism, oxidative capacity, contraction speed, fibre size, ATPase activity, myoglobin and glycogen content as well as an increased glycolytic potential (Choe *et al.*, 2008, Choe & Kim, 2014). Therefore, the direct comparison of studies determining the early post mortem metabolic status of pork using Raman spectroscopy (Pedersen *et al.*, 2003, Scheier *et al.*, 2014) with the current study is further complicated as pH and temperatures in this study were measured at 25 m post- mortem and 24 hours post mortem as well as a final pHu measurement after 5 days and so it is not possible to determine the rate of pH decline.

Like rapid pH decline, the development of low pHu has been related to high purge (Pearce *et al.*,

2011). It is hypothesised that both accelerated pH decline and low pHu cause greater purge as there is a higher amount of protein denaturation, particularly if temperatures are higher at the development of pHu, as a result of cell structural changes which facilitate the movement of immobilised water through extracellular spaces (Huff Lonergan & Lonergan, 2005, Pearce *et al.*, 2011). Once the pH of the muscle post mortem reaches the isoelectric point of the major proteins, the repulsion of the structures within the myofibril is reduced causing them to pack closer together, reducing space (Huff Lonergan & Lonergan, 2005, Puolanne & Halonen, 2010).

In conjunction with these changes, formation of actin and myosin cross bridges and any shortening of the sarcomere as the muscle enters rigor results in longitudinal and lateral contractions, further reducing the space in the myofibril available for water (Tornberg, 1996). Consequently, immobilised water may be forced into extracellular compartments resulting in it being lost as purge (Pearce *et al.*, 2011).

Data in this study also demonstrated that there is the potential to use Raman spectroscopy to predict *L** (meat lightness) at 24 h and 5 days post mortem as models yielded cross validated correlations between predicted and observed values (R^2_{cv}) of 0.32 and 0.22, respectively. This prediction using Raman spectra also gave reductions in the error of the prediction ($RMSEP_{cv}$) of 20% at 24 hours PM and of 12% at 5 days PM.

The structural approach to understanding interactions between colour, water holding capacity and tenderness taken by Hughes *et al.* (2014) highlights the links between these structural changes related to the metabolic processes through the development of rigor, water holding capacity and colour. Therefore, the prediction of *L** using Raman spectroscopy may be based on some of the same biochemical and biophysical characteristics established during early post mortem metabolism which determine purge and pH values.

Factors which alter the structure of the muscle, including shrinkage of the myofibril, interfilament spacing, development of extracellular spaces and protein denaturation affect water holding capacity as well as the reflectance of light (Hughes *et al.*, 2014) and consequently lightness, which is measured by the *L** value (Priolo *et al.*, 2001). This occurs as the scattering of light within the microstructure effects how much light is transmitted into the depth of the muscle and how much is reflected. However, the reflectance of light is also a function of the abilities of different components within the meat to scatter entering light and their concentrations within the meat. Hence, lightness is also defined by other factors including myofibrillar size and density, striations of the muscle as well as amount and distribution of water, intramuscular fat and connective tissue (Hughes *et al.*, 2014).

Given that the hand held device also uses the scattering of light to determine the biochemical and physical properties of meat (Schmidt *et al.*, 2009) it could be hypothesised that *L** values should have a higher correlation with Raman spectroscopic measurements than those found in this study. However, prediction accuracy of *L** values using Raman spectroscopy could be reduced for samples with higher pH, darker meat, tighter myofibrillar structure or a denser myofibrillar mass as a result of lowered scattering properties. This is the result of a greater loss of back scattered light to absorption as it traverses the meat, since the photons interact with more particles before being reflected at the surface. Due to the longer path light takes to pass through the meat, less light is reflected back and the meat appears darker (Hughes *et al.*, 2014). Whilst a reduction in overall intensity would facilitate the prediction of darker meats due to the biophysical properties and

increased absorption causing reduction in Raman signals present in spectra (McCreery, 2005), there would also be less information on the biochemical characteristics of the meat.

It is hypothesised that these factors which explain some variation in $L*$ values may also explain some of the variation in prediction outcomes in Raman spectroscopic studies between species. If samples with lighter $L*$ values have better scattering properties (Hughes *et al.*, 2014) prediction of meat quality of pork using Raman spectra could be more accurate than darker meats such as beef and lamb, as more biochemical information will be contained in spectra. However, as beef has a larger myofibrillar size in comparison to lamb, more spectroscopic information will also be contained in spectra collected from beef as it will have greater light scattering properties. Furthermore, the reduction in absorption losses from lighter or less structurally dense samples could result in more information in spectra from deeper areas of the tissue as McCreery (2005) and Matousek & Stone (2009) suggest that optically dense samples have a shorter sampling depths.

Given that Pedersen *et al.* (2003) found that increasing baseline and fluorescence in reference spectra was caused by the trace components of glycogens and the high absorbance properties of myoglobin prevented them from obtaining a reference spectra, it is plausible that the muscle and muscle face used for Raman spectroscopic measurement also has an impact on the scattering properties. This may be a consequence of muscle fibre type and muscle type as glycogen content, capillary density, oxidative capacity and z-line width vary with muscle fibre type (te Pas *et al.*, 2004) and the intra and inter muscular variation of muscle fibre type (Klont *et al.*, 1998). Therefore, some muscles or muscles from some species may have a better ability to scatter the Raman signal providing a better prediction of meat quality traits. However, further research is needed to determine the impact of species and muscle differences on light scattering properties and subsequent Raman spectra.

Based on the ranges of meat quality indicators and prediction models found in this study lamb and sheep meat industries could significantly benefit from further developing Raman spectroscopy as a non-invasive single tool for the prediction of carcasses which deviate in metabolic processes and consequently pH, purge and $L*$ values. Given that up to 6.4% of the weight of the product was lost as purge after 5 days ageing and most lamb SMs fell below the $L*$ value of 44 outlined by Khliji *et al.* (2010) to be acceptable to 95% of consumers, better classification of product which falls into these categories would enable processors to make earlier decisions on the suitability of carcasses to match specifications and the consumer expectations in both export and domestic markets. However, these results are yet to be validated and these findings are limited to lamb. Identification of carcasses which deviate from the normal metabolic processes and consequently metabolic related meat quality traits may be more advantageous in identifying beef carcasses which are susceptible to conditions such as dark firm and dry (DFD) meat and heat shortening.

Conclusion

This study demonstrated the potential to use Raman spectra collected at 1 day post mortem to predict pHu, pH$_{24}$, purge and $L*$ measured at 1 and 5 days post mortem on fresh intact lamb. Although it is not practical to use a spectroscopic technology to predict only pH values given that a pH meter is a cheaper more robust option, there may be a benefit to industry from predicting purge loss using Raman spectra as the accuracy was improved compared to using pHu alone. Furthermore, this study suggests that there may be an ability to predict pHu, pH$_{24}$, purge and $L*$ values from a single measurement at 24 h which does not penetrate the muscle as a pH probe does.

Due to the established relationships between colour, water holding capacity, pH decline and pHu, it is hypothesised that Raman spectroscopy is able to predict meat quality indicators which relate to the post mortem metabolic processes. As this is the first study which reports the prediction of other meat quality traits, further research is required to determine whether these predictions are repeatable.

3.2.3 Prediction of Other Meat Quality Traits – Intramuscular fat and major fatty acid group composition

Materials and Methods: Samples

At 1 day post mortem (PM), the cranial portion of *m. longissimus lumborum* (LL; Product identification number HAM 4866; Anonymous, 2005) was collected from 80 lamb carcasses over 4 consecutive days (20 per day) from the same abattoir. Samples were randomly selected from different consignments of unknown origins and therefore unknown backgrounds, age and gender, to represent the various animals typically processed by the abattoir, in order to obtain a spread in the levels of IMF and different FA composition. The same carcasses were used for the experiments reported in objective 1 (experiment 1). Sample weights of three LL portions were too small to provide adequate sample for FA reference analysis and thus these samples were not further considered.

Raman spectroscopy

Raman Spectroscopic measurements were conducted at 24 h PM using a Raman hand held probe (Schmidt *et al*., 2009) with a 70mW laser, an integration time of 3.45 s and 1 accumulation as shown in Figure 11. Ten Raman scans were taken on each cranial portion at ambient temperature on chilled LL samples. Once RS measurement was complete, the portion was frozen and held at -20°C until subsequent analysis of fatty acids.

Figure 11. Hand held Raman Spectroscopy sensor head measuring the cranial portion of a fresh intact lamb LL with the epimysium removed, perpendicular to the muscle fibres.

Intramuscular Fat and Fatty Acid Analysis

After being frozen and stored at -20°C until analysis, the cranial portion of LL was freeze dried and homogenised prior to measurement. Reference measurements for IMF were conducted using the Soxhlet method (AOAC, 1992) adapted by removing the use of sand and cotton during determination and 40 ml of hexane was used as the extraction solvent. Once extracted the mixture was dried for 30 min at 105 °C prior to being cooled and weighed. The quality assurance method applied to this measurement is based on checks for 20% of samples, based on undertaking repeats.

A rapid modified procedure adapted from Folch *et al.* (1957) was used to extract and methylate the FAs, as described in full by Ponnampalam *et al.* (2014). For each muscle sample, an internal standard (nonadecanoic acid methyl ester; C19:0, Sigma Aldrich Pty Ltd, Castle Hill, NSW 2154, Australia) was added to verify the precision of the estimates. Individual fatty acids quantified by capillary GC (HP INNOWAX 60 m×0.25 mm, 0.5 μm, Agilent J&W Scientific, Santa Clara, CA, USA) were identified using a reference standard (Supelco C4-C24 mix, Sigma Aldrich Pty Ltd, NSW 2154, Australia), which was run in each batch.

Data Analysis

A measurement was taken of the sample without the laser on to determine the contribution of background noise, which was subtracted from the spectra before they were saved as raw data. Fat spectra were identified at time of measurement by the software that operates the Raman hand held probe and spectrograph and saves the Raman spectra (Schmidt *et al.*, 2013). After measurement, fat spectra were further analysed using PCA with the lipid and protein spectral patterns as components to identify spectra which contained only Raman signals relating to lipids for chemometric analysis. Spectra for each sample were then averaged and reduced to wavelength frequencies at 500 – 1800 cm^{-1}.

Models to predict IMF and the major FA groups were fitted using Partial Least Squares (PLS) with k- fold (k = 8) cross validation to determine the optimal number of latent variables to include, as previously described for experiment 1 under objectives 1 and 2.

Key traits including IMF levels and concentrations of polyunsaturated fatty acids (PUFA), monounsaturated fatty acids (MUFA), total unsaturated fatty acids (USFA = MUFA + PUFA) and saturated fatty acids (SFA) were calculated as the sum of the FAs (mg/ 100 g meat) relevant to the specific category of the 27 individual FAs quantified by capillary gas chromatography (GC). Furthermore, the sum of these 27 individual FAs quantified by GC was calculated to determine total identified fatty acids. These categories were then used as model covariates. Several approaches were tried to account for the interactions between IMF and FA composition traits. These included incorporating IMF into the prediction using IMF amount (g/100g) as an additional model covariate and calculation of the FA group traits as percentage of IMF (Eq. 1) where *i* equals the *i*th sample from 1 to 77.

$$FA\% = (FA^i \text{ (mg/100 muscle)}/IMF^i \text{ (mg/100 muscle)} \times 100/1) \qquad \text{(Eq. 1)}$$

Results

Within this study, IMF levels ranged from 2.0 – 7.7 g/100g meat (mean 4.0 ± s.d. 1.1). Summary statistics for FA composition are described in Table 14.

Table 15. Summary statistics of lamb *m. longissimus lumborum* FA composition (mg /100g meat).

Fatty Acid (mg/ 100g)	Mean (± s.d)	Range (min, max)
Individual Fatty Acids		
14:0	96.3 ± 32.1	33.1 – 171.1
16:0	824.8 ± 207.5	411.6 – 1437.5
18:0	582.1 ± 157.4	257.5 – 1045.0
14:0 + 16:0	921.1 ± 234.8	444.7 – 1597.7
18:1(Δ 9)	1442.5 ± 396.2	721.2 – 2585.2
18:2 n-6	156.2 ± 30.7	94.5 – 241.5
20:4 n-6	37.7 ± 6.9	24.3 – 55.4
Total n-6	198.3 ± 35.5	127.7 – 287.4
18:3 n-3 (ALA)	65.5 ± 15.9	34.6 – 113.9
20: 5 n-3 (EPA)	25.8 ± 3.1	16.6 – 31.6
22: 5 n-3 (DPA)	30.9 ± 2.8	22.8 – 36.0
22: 6 n-3 (DHA)	8.8 ± 2.1	5.4 – 15.3
EPA + DHA	34.7 ± 4.1	23.6 – 45.2
EPA + DHA + DPA	65.5 ± 5.6	47.8 – 79.2
Major Fatty Acid Groups		
Total Omega- 6	198.3 ± 35.5	127.6 – 287.4
Total Omega- 3	131.6 ± 19.7	93.2 – 185.2
PUFA	333.4 ± 50.2	235.7 – 477.3
MUFA	1515.7 ± 414.2	757.1 – 2704.4
USFA	1849.1 ± 430.7	1065.1 – 3101.5
SFA	1568.0 ± 398.4	735.1 – 2761.1
Omega-3: Omega- 6	0.68 ± 0.11	0.42 – 0.99
PUFA: SFA	0.22 ± 0.06	0.13 – 0.44
Total identified fatty acids (TIFA)	3415.4 ± 816.9	1837.2 – 5676.9
Extraction Efficiency (%)	85.5 ± 5.9	73.4 – 108.6

Comparing the concentrations of major fatty acid groups extracted using the two-step procedure to IMF level (Fig. 12) demonstrates that concentrations of MUFA and SFA were strongly correlated to increasing IMF levels (R^2 = 0.91 and 0.92, respectively), while PUFA remained constant despite increasing IMF levels (R^2 = 0.15).
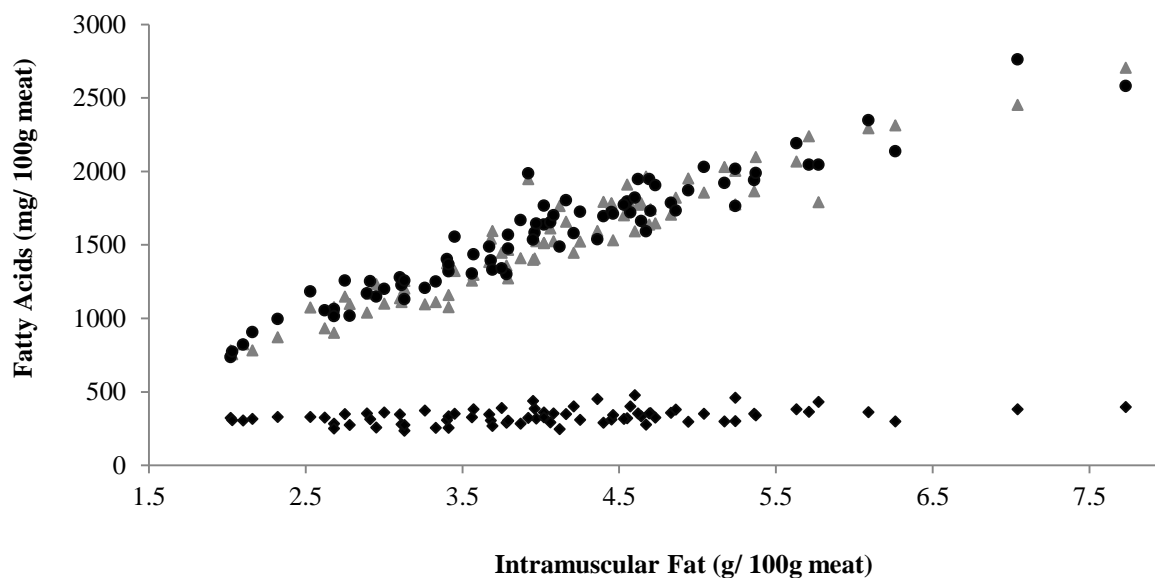

Figure. 12 Correlation between Intramuscular fat (g/ 100g) of lamb *m. longissimus lumborum* and polyunsaturated fatty acids (mg/ 100g; diamonds; R^2 = 0.15), monounsaturated fatty acids (mg/ 100g; triangles; R^2 = 0.92) and saturated fatty acids (mg/ 100g; circles; R^2 = 0.91).

The results of the chemometric analysis (Table 15) indicate that the error of the prediction was reduced when the major FA groups were predicted using Raman spectra (optimal RMSECV) for all key traits (relative reductions in RMSECV 0.3% – 40.8%), except for the ratio of PUFA: SFA. The relationships between predicted and observed values (R^2) were best for the unsaturated FAs as prediction of PUFA yielded an R^2 of 0.93 using Raman spectra, while prediction of MUFA gave an R^2 of 0.54. It is interesting to note that these R^2 values were reduced when the relationships were cross-validated (R^2_{cv} = 0.21 PUFA; R^2_{cv} = 0.16 MUFA).

Table 16 Results of chemometric analysis for the prediction of intramuscular fat (IMF) (g/ 100 g of meat) and the major fatty acid (FA) groups (mg/100 g of meat) including the relationships between predicted and observed values (R^2), cross-validated correlation between predicted and observed values (R^2_{cv}) the optimal and null root mean square error of cross validation (RMSECV; mg/100g) and the relative reduction in RMSECV (%).

Fatty acid groups	R^2	R^2_{cv}	Null RMSECV	Optimal RMSECV (latent variables)	Reduction in RMSECV
IMF	0.08	0.02	1.14	1.12 (2)	1.8
MUFA	0.54	0.16	416.89	400.30 (7)	4.0
PUFA	0.93	0.21	50.50	46.57 (11)	7.8
USFA	0.08	0.01	433.51	432.32 (2)	0.3
SFA	0.08	0.01	401.00	358.72 (2)	11.0
PUFA: SFA	0.21	0.13	0.06	0.06 (2)	0.0
Total Identified FA	0.07	0.01	1382.11	818.69 (2)	40.8

Overall the best prediction model, based on the relative reduction in RMSECV and the coefficient of determination, was for PUFA. This model yielded a 7.8% reduction in RMSECV and R^2 = 0.93 and R^2_{cv} = 0.21 respectively (Fig. 13). However, this model is based on a high number of latent variables (11 LV; Table 15).
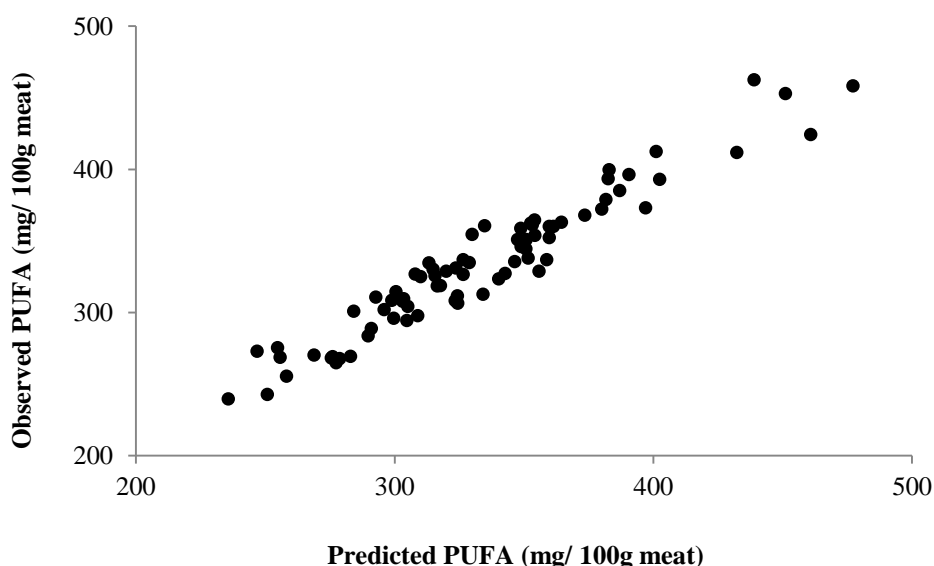

Figure 13. **Polyunsaturated fatty acids (PUFA) in *M. longissimus lumborum* (mg/ 100 g meat) predicted using Raman spectra compared to observed values (optimal root mean square error of cross validation (RMSECV) = 46.57, R^2 = 0.93, R^2_{cv} = 0.21).**

As evident in Table 16, the prediction of SFA was improved by calculating SFA as a percentage of total IMF, which yielded an R^2 = 0.56 and an R^2_{cv} = 0.31. It is interesting to note that while calculating FA groups as a percentage of IMF to remove the impact of the strong relationship between IMF and MUFA did not improve the co-efficient of determination (R^2 = 0.54 to 0.00), it did improve the cross-validated co-efficient of determination to R^2_{cv} = 0.20.

Table 17 Summary chemometric analysis for the prediction of key fatty acid (FA) composition groups of ovine *M. Longissimus lumborum* comparing the fatty acid group as a percentage of intramuscular fat (FA %)* and incorporating intramuscular fat as a covariate with Raman spectra in the prediction model (RS + IMF) to account for the interactions between IMF levels and major FA groups.

Fatty Acid Traits (mg/ 100g meat)	Observed FA		RS + IMF		FA %[*]	
	R^2	R^2_{cv}	R^2	R^2_{cv}	R^2	R^2_{cv}
MUFA	0.54	0.16	0.54	0.16	0.00	0.20
SFA	0.08	0.01	0.08	0.01	0.56	0.31

[*] FA% = [FAi (mg/100 muscle)/IMFi (mg/100 muscle) × 100/1]   (Eq. 1)

Discussion

The IMF level found in this study is consistent with the levels expected in retail lamb in Australia. Previous studies have reported mean IMF values for lamb loin (both *m. longissimus thoracis* and *m. longissimus lumborum*) in Australia of between 3.4 – 5.3% (Ponnampalam *et al.*, 2001a, Ponnampalam *et al.*, 2001b, Pannier *et al.*, 2014). In regard to human health targets the ranges found demonstrate that on average the lamb in this study would meet the nutritional requirements to be identified as being a good source of omega-3 fatty acids as it contains not more than 5g /100 g of SFAs and contains more than 30 mg/ 100g of either DHA or EPA (Food Standards Australia New Zealand, 2012).

Overall, this study indicates that there is potential to predict the concentration of PUFA extracted using the two-step procedure using Raman spectroscopy. This prediction was found to be more accurate than that in intact salmon (Afseth *et al.*, 2006). Using a ball probe attached to a Raman spectroscopic instrument via a fibre optic cable, Afseth *et al.* (2006) found that multivariate correlations of R = 0.67 and 0.73 were achievable for prediction of the iodine value of the intact dark muscle from salmon. However, this was improved to r = 0.86, when the salmon samples were ground. Afseth *et al.* (2006) proposed the differences in multivariate correlation coefficients between ground and intact samples were the result of sampling differences that resulted in a mismatch between reference measurements and the spectra of intact samples, as spectral measurements and reference analysis were conducted on separate halves of the same portion of the fish. The present study avoided these issues with sampling by conducting Raman spectral measurements on the same portion of muscle which was then freeze dried and ground for reference measurement and thus the accuracy of the prediction was improved. Although, the prediction of FA composition may be further improved by grinding the samples prior to Raman Spectroscopic scanning to remove the errors associated with measuring a complex heterogeneous sample, this would remove the advantages of using Raman spectroscopy as a non-destructive tool for FA determination in commercial applications.

While a limited ability to predict MUFA was also found in this study and SFA which had been adjusted for its strong correlation with IMF, there was no potential to predict any other FA trait or IMF level. Being the first study to determine the potential of Raman spectra to predict the IMF level and FA composition of fresh intact ovine muscle *in- situ*, no literature exists with which to compare the methods, chemometric analysis and thus the results of this study.

Other previous studies using Raman spectroscopy to predict the FA composition of porcine adipose tissue (Olsen *et al.*, 2007, Olsen *et al.*, 2010) have indicated that FA composition was able to be predicted with good accuracy (cross validated coefficients ranged from 0.95 – 0.98). However, measuring adipose tissue these studies avoided the need to discriminate between meat and fat spectra to remove contributions from overlapping protein vibrations on the lipid signals which can arise during the measurement of IMF levels in-situ. With previous work that determined the ability of Raman spectroscopy to predict the tenderness of intact ovine *longissimus lumborum* muscles from the same carcasses (experiment 1, objectives 1 and 2), the method to discriminate between lipid and protein spectra was already established. This was established using the hand held Raman device that had previously been developed to assess the quality of pork (Schmidt *et al.*, 2009). This process uses PCA to identify lipid contributions to the spectra by comparing key vibrations in each spectra with saved components (Schmidt *et al.*, 2010). As pork subcutaneous adipose tissue is higher in long chain PUFAs in comparison to lamb (Wood *et al.*, 2008) and RS is sensitive to species differences in FA composition (Beattie *et al.*, 2007), it is plausible that this process may have affected prediction models. Therefore, prediction outcomes may be improved by creating a PCA model for discrimination between protein and lipid spectra which uses species specific spectra of intramuscular fat as the saved components.

Furthermore, this approach of discriminating between lipid and protein spectra does not distinguish between spectra containing only lipid signals and spectra containing mixed lipid and protein signals. Removing all spectra that contain mixed lipid and protein signals not only significantly reduces the number of spectra available for analysis, but may also remove information on the lipids bound in membranes. Consequently, further research is required to determine the best threshold to filter spectra with mixed lipid and protein signals. Improving this discrimination between spectra could be achieved by quantifying the concentration of fat detected in the spectra. Using the surface area of the window of the hand held device and the depth of the laser focus combined with the intensities of the lipid peaks in the spectral data, it would be possible to calculate the percentage of the muscle area measured which includes contributions from lipids. Therefore, spectra with increasing contributions of protein bands could be saved separately facilitating a better distinction between 'bad' lipid spectra (e.g. noisy or highly fluorescent spectra containing only lipid signals) and spectra which have increasing contributions of proteins or increasing proportions of lipids. Furthermore, improving the discrimination of spectra containing mixed protein and lipid signals could also increase the potential to predict IMF levels in intact muscle.

Fatty acids in IMF are different to fatty acids in adipose tissue as they consist of triglycerides in adipocytes as well as phospholipids in the membranes of the myofibril (te Pas *et al.*, 2004). This difference in lipid fractions could account for the poorer prediction of SFA and MUFA as well as the decrease in prediction co-efficient correlations when cross-validated as found in this study, given phospholipids have a more complex chemical structure. Hence, the spectral assignments and predictions previously described for triglycerides (Olsen *et al.*, 2007, Olsen *et al.*, 2010, Lyndgaard *et al.*, 2011) and simplified FA mixtures (Beattie *et al.*, 2004a, Afseth *et al.*, 2005) may not correlate with those of phospholipids deposited in red meat.

In contrast to the relatively simple structure of triglycerides, phospholipids consist of two FA chains covalently bonded to a glycerol molecule, a phosphate group and another molecule, which determines the phospholipid type (Nelson & Cox, 2008). For example, phosphatidyl choline has CH_2 groups and C-C bonds in the choline molecule which forms part of its hydrophilic head. During excitation these bonds have the same vibration as the CH_2 groups and C-C bonds present in the fatty acid side chains. Consequently, Raman spectra from phospholipids have overlapping contributions from other chemical bonds in the hydrophilic head within the same wavenumbers used to determine FA composition (Wallach *et al.*, 1979). This is a unique limitation to the application of Raman Spectroscopy for IMF *in-situ* prediction within fresh intact muscle, as Raman Spectroscopy studies conducted on simplified phospholipids in laboratory conditions can use greater wavenumbers (e.g. 2900 – 3200 cm^{-1}) which partly avoids these overlaps (Larsson & Rand, 1973, Lis *et al.*, 1976, Bunow & Levin, 1977, Susi *et al.*, 1979). However, the hand held Raman device used in this study has been designed to measure meat that gives a weak Raman signal so shorter measurement times and an excitation wavelength to reduce the generation of fluorescence while maintaining the efficiency of detectors is required (Schmidt *et al.*, 2009). Hence, the spectral range of this study is restricted to 500 – 2100 cm^{-1} and these larger wavenumbers have not been measured.

If overlap of the CH_2 group and the C-C bond vibrations of the hydrophilic head of phospholipids are present when RS is conducted *in-situ*, they would contribute to predicted fatty acid values. However, as they do not form part of the FA chains and are removed during the methylation and extraction of FAME for FA analysis, they are not accounted for in the observed FA values. As a result there would be a reduction in the correlation between predicted and observed FA values. Furthermore, it is plausible that the random selection of carcasses sampled to obtain LLs with a range of IMF levels and FA compositions has resulted in varying contributions of phospholipids to the fat spectra, as increasing IMF levels increases the amount of triglycerides within the muscle, while phospholipids remain constant (te Pas *et al.*, 2004). Consequently, LL portions with lower levels of IMF may be more affected by this spectral overlap effect of the CH_2 and C-C vibrations compared to LL portions with higher levels of IMF. This may create an over or underestimation of the FA group concentrations causing reductions in the correlation of predicted and observed values that occurred when models were cross validated.

Based on this research, further study into the relationships between IMF, lipid fractions and FA composition in ruminants is warranted. It is likely that PUFA in lamb is mainly bound in the phospholipid fraction, similarly to pork, beef, rabbit and poultry (Hernández *et al.*, 1998, te Pas *et al.*, 2004), given that the proportion of phospholipids present in the muscle remains constant regardless of IMF levels, as did PUFA within this study. However, as SFA and MUFA were strongly correlated with increasing IMF and adjustment for IMF levels significantly improved the predictive ability of SFA, there may also be a correlation between the quantity of triglycerides and FA composition in lamb LL. Therefore, a greater understanding of the interactions between proportions of lipid fractions, IMF levels and FA composition of ruminants is required. This information is also needed to provide better insight into the chemical structure of FAs *in-situ* within the myofibrillar matrix and the links between chemical bonds of lipids and FA which would provide a better approach for the prediction of FA composition using technologies such as RS. However, there are larger implications of the correlations between IMF, lipid fractions and FA composition, as the polarity of the lipid fraction affects the extraction and recovery of FA (Clayton *et al.*, 2012) as well as the oxidation and retail shelf life of meat products (Ponnampalam *et al.*, 2001b).

Conclusion

Overall this study demonstrated that there is potential for Raman spectroscopy to predict the PUFA, MUFA major FA groups and SFA as a percentage of IMF. However, there is currently no opportunity to compare these results with other studies using Raman spectroscopy to predict major FA groups and IMF level *in-situ* within fresh intact muscle. Thus, validation of the accuracy and prediction errors found in this study is required.

This study also suggests that the prediction of fatty acid composition may be improved by further developing the differentiation of lipid spectra from protein spectra. By developing models to differentiate spectra based on signals of lamb, any potential for bias in the selection of spectra for further analysis would be removed which could increase prediction outcomes.

3.2.4 Biochemical and Biophysical Characteristics

Although changes in the Raman spectra were identified with ageing and differences in shear force values during these experiments, poor prediction models suggests that there is little significant difference between the spectra or there is significant background noise and variation in spectra which does not contribute to prediction models. Therefore, understanding the spectra by completing spectral interpretation on these models is not informative in terms of determining what biochemical and biophysical characteristics are underlying the predictions. Consequently, this section will focus on the interpretation of spectra that underlie the predictions of purge, pH and polyunsaturated fatty acids to understand what biochemical and biophysical characteristics are contributing to these predictions. Further interpretation of spectra in relation to tenderness is outlined in full in the PhD thesis and published papers, which includes a Raman microscopic study to further understand the links between the biophysical characteristics of the myofibril and the spectra.

3.2.4.1 Purge

A tentative band assignment of spectra from SMs with the highest and lowest purge suggests that differences between SMs are complex, however it does support the hypothesis that changes in purge are related metabolic processes in the conversion from muscle to meat and subsequent structural changes. Spectra obtained from SMs with high purge demonstrate an overall reduction in intensities at key wavenumbers including 716, 750, 822, 852, 870, 930, 1044, 1076, 1308, 1448, 1611 and 1650 cm^{-1} (Fig. 14). Furthermore, there are increases evident in the region between 500 – 700 cm^{-1} and in Raman signals at 716, 750, 1332, and 1567cm^{-1}.
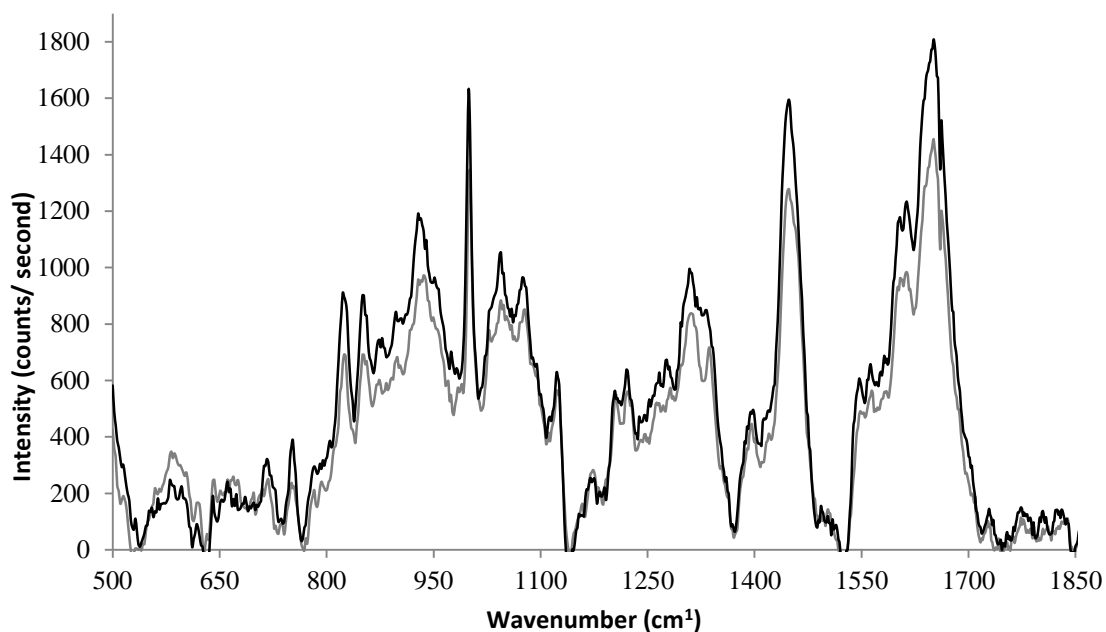
Figure 14. The averaged and background corrected spectra collected at 24 hours post mortem from the ovine *m. semimembranosus* with the 5 highest (4.65 – 6.42; grey) and lowest purge (1.10 – 1.23; black).

Although these changes are complex and the impact of overlapping signals is unknown, the decreases in intensity at 580, 870, 890, 930, 1044, 1076, 1308 and 1332 cm^{-1} are similar to changes evident in spectra from high pHu values further agreeing with the correlation that indicates purge increases with increasing pHu. Previous band assignments completed for changes in pHu identifies several of these changes suggesting that with increasing pHu and purge there is a reduction in inorganic phosphate (875 cm^{-1} and 1044 cm^{-1}), α- helical proteins (930 cm^{-1}), CH deformation signals (1448 cm^{-1}) and COO^{-} signals (Scheier *et al.*, 2014) present in spectra collected at 24 hours post mortem. Raman spectra synthesised by Pedersen *et al.* (2003) for pure components present in meat provides further insight to spectral changes associated with variation in water holding capacity of meat suggesting that the peak evident at 852 cm^{-1} could be characteristic of α- glucans, the pyrrolidine ring of hydroxyproline a main component of collagen or part of the lactate signal that was found to be split across three wavenumbers (850, 1330 and 1460 cm^{-1}). Furthermore, peaks at 940 cm^{-1}, 1320 cm^{-1} and 1450 cm^{-1} were identified as α- helical protein conformation, the CH bend and the symmetric methylene bend associated with myofibrillar proteins, while the peak at 820 cm^{-1} was determined to be a reflection of the phosphate group in ATP (Pedersen *et al.*, 2003). Tentative band assignments on the remaining Raman spectral changes suggest that spectra from SMs with high purge may also be characterised by a decrease in adenine (716 cm^{-1}), lactic acid (750 cm^{-1}), inorganic phosphate (580 cm^{-1} and 1076 cm^{-1}), phosphodiesters (822 cm^{-1}) and glycogen (852 cm^{-1}) (Movasaghi *et al.*, 2007).

Overall these spectral changes agree with the conclusion of Pedersen *et al.* (2003) that the changes in Raman spectra are consistent with the relationship between water holding capacity and pH, glycogen concentration and protein conformations already established in existing literature. However, it is difficult to compare spectral assignments directly with Pedersen *et al.* (2003) as their interpretation is not detailed as there were few samples measured with Raman microscopy. Using the findings for high pHu values suggests that those samples with higher purge may have reached

pHu values earlier and therefore may enter rigor at slightly higher temperatures causing greater amounts of protein degradation (Huff Lonergan & Lonergan, 2005) as evident in the increased signals associated with amino acid side chains between 500 – 700 cm^{-1} (Scheier *et al.*, 2014) and a lower overall intensity of signal due to increased diffuse scattering of excitation photons within the myofibril (Matousek & Stone, 2009). Although it could be considered that reaching pHu earlier should demonstrate an increase for the Raman signals of inorganic phosphate, adenine and lactate as well as a decrease signals for glycogen (Scheier *et al.*, 2014), the decreased intensities found in this study may be indicative of lower glycogen and ATP concentrations in the muscle at slaughter. Consequently, the rate of pH decline may not be different yet the extent of anaerobic glycolysis post mortem would be reduced resulting in higher pHu (Choe *et al.*, 2008) and potentially higher temperatures at rigor (Savell *et al.*, 2005). However, as with the prediction pHu values previously discussed, due to the lack of extreme pH values in this study and the ambiguity of spectral assignments as a result of the potentially overlapping bands, the exact biochemical pathways behind the variation in purge are unknown. Therefore, future research in Raman spectroscopy needs to address this.

3.2.4.2 pH

Elucidating the underlying spectra for the prediction of the highest and lowest pHu values of lamb SM illustrates the complexity of the spectral changes, as differences are present in Raman signals between 563 – 720 cm^{-1} with clearer differences at 585 cm^{-1}, as well as at 937 cm^{-1}, 1042 cm^{-1}, 1076 cm^{-1}, 1124 cm^{-1}, 1206 cm^{-1}. Furthermore, smaller differences are evident at 1175 cm^{-1}, 1134 cm^{-1}, 1562 cm^{-1} and 1611 cm^{-1} (Fig. 15).
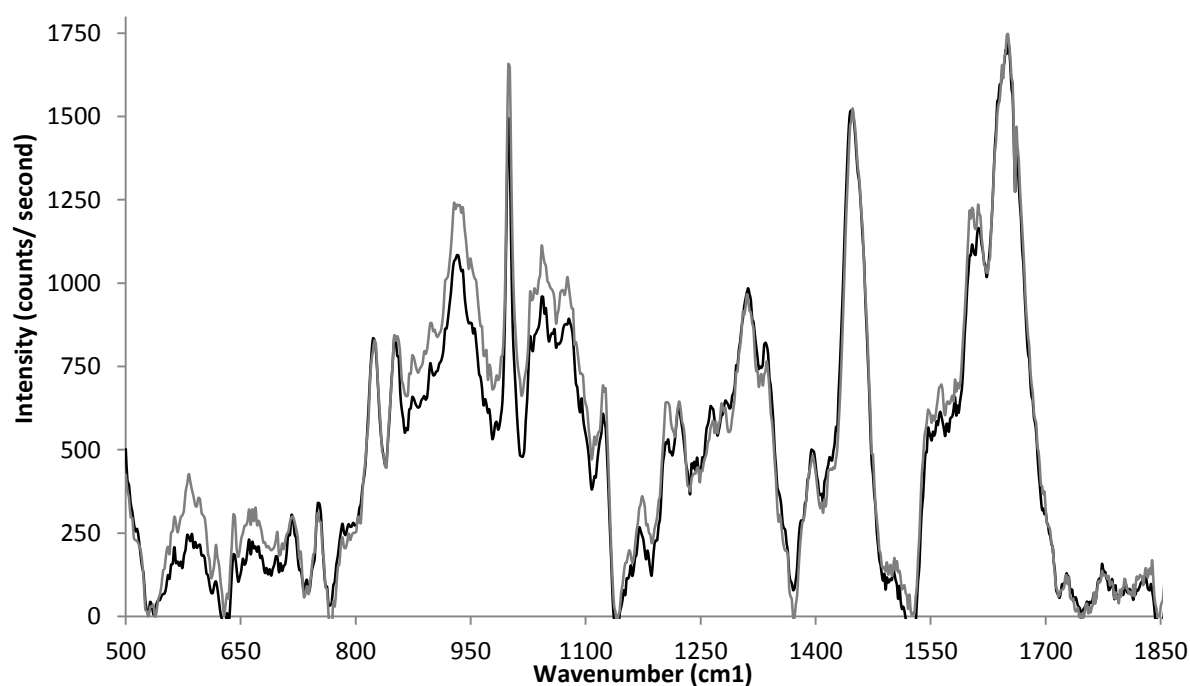

Figure 15. The averaged background corrected Raman spectra collected 24 hours post mortem from the ovine *m. semimembransous* with the 5 highest (5.90 – 6.16; black) and lowest (5.59 – 5.61; grey) pHu values.

While some spectral assignments can be made based on the research of Scheier *et al.* (2014), it must be stressed that pHu is a measure of the extent of pH decline while the rate of pH decline is dependent on the metabolic rates (Choe & Kim, 2014) which was measured by Scheier *et al.* (2014) in terms of metabolites present during the on-set of rigor. As porcine muscle contains more type IIB muscle fibres then lamb (Kerth, 2013) and therefore has different biochemistry characteristics including oxidative and glycolytic capacity, contraction speed and glycogen content (Choe *et al.*, 2008), it can be expected that there would be differences in spectra evident in the pH decline of pork and lamb pHu measured at 24 hr post mortem which may limit the transfer of findings between these two studies.

Of the major changes in peak intensities present in spectra from samples with low and high pHu values, those that can be potentially identified using the previous study on pH decline in pork (Scheier *et al.*, 2014), include the increases in intensity at 875 cm^{-1}, 937 cm^{-1}, 1042 cm^{-1}, 1334 cm^{-1}, 1567 cm^{-1} and the numerous small changes within the region between 563 – 720 cm^{-1}.

Overall these shifts suggest that SMs with low pHu values had increased concentrations of inorganic phosphate (875 cm^{-1}, 970 cm^{-1} and 1042 cm^{-1}), adenine (1334 cm^{-1}), α – helical proteins (937 cm^{-1}) and more significant changes to amino acid side chains (563 – 720 cm^{-1}) (Scheier *et al.*, 2014). This may indicate that lamb SMs with lower pHu values have a higher concentration of glycogen in the muscle post mortem and therefore reach a more advanced stage of anaerobic glycolysis in 24 h post mortem compared to SMs with higher pHu values. This is because higher levels of inorganic phosphate (England *et al.*, 2013) and lactate (te Pas *et al.*, 2004), as well as greater changes to α- helical proteins such as actin and myosin (Huff Lonergan *et al.*, 2010) and larger amounts of protein denaturation (Huff Lonergan & Lonergan, 2005) have all been associated with the completion of anaerobic glycolysis.

Although these Raman signals suggest increases in inorganic phosphate and α-helical proteins are linked to low pHu, it is unclear what exactly biochemical pathways cause the relationships between these intensities and the free H^+ that is measured by the pH reference measurement. Inorganic phosphate is a key element within many post mortem processes, including the breakdown of phosphocreatine, the synthesis and breakdown of glucose-6 phosphate and sugar phosphates, anaerobic glycolysis, formation and detachment of actin/myosin cross bridges and re-activation of myosin during muscular contraction (te Pas *et al.*, 2004). Furthermore, there are many α- helical proteins present in meat, including tropomyosin, myosin and actin, and the intensity of Raman signals relating to these α- helical proteins is dependent on concentration as well as sample orientation (Pézolet *et al.*, 1988). As a result, changes to the orientation of the collagen matrix (Nakamura *et al.*, 2010), formation of more actomyosin cross bridges, changes to the orientation of myosin as the attached myosin heads pivot and shorten the sarcomere (te Pas *et al.*, 2004) or higher concentrations of glycogen and glucose still within the cells as the muscle enters rigor may account for differences in the signal pertaining to α-helical proteins. Consequently, it is difficult to determine which of these biochemical processes are vital in determining the increase in peak intensities measured in SMs with lower pHu at 24 h PM.

Comparing the averaged background corrected spectra collected at 24 h PM from the samples with the lowest pH_{24} and the lowest pHu values demonstrate that there are no major changes between 24 h and 5 days post mortem. As illustrated in Figure 16, there are minor changes at 582, 875,
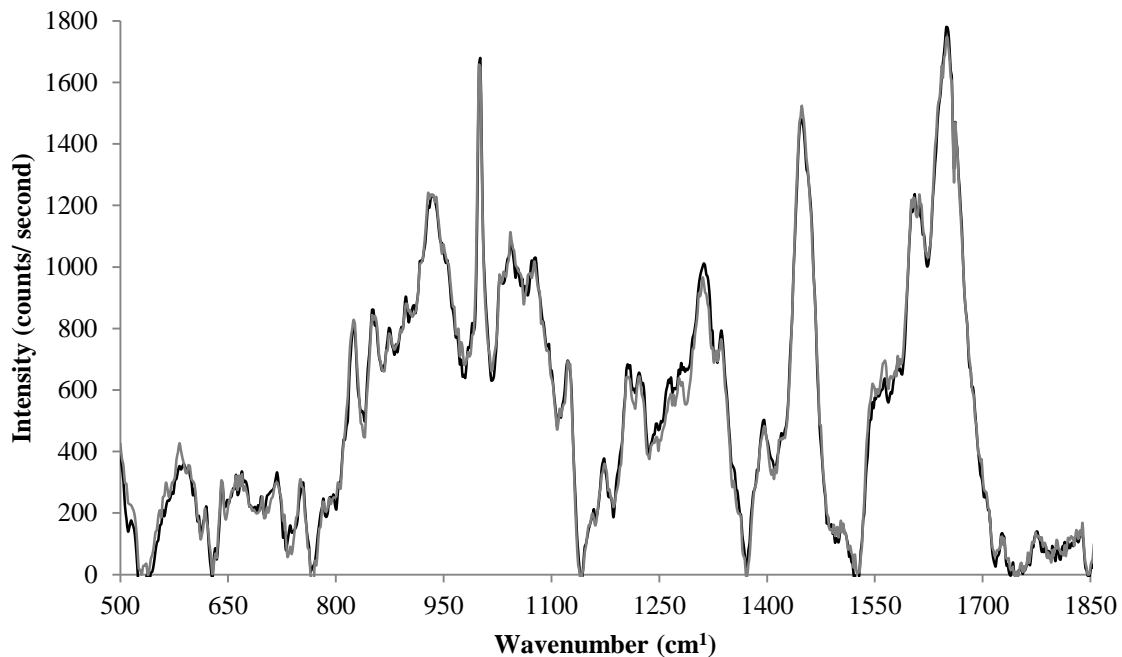
1205, 1222, 1255, 1261, 1278, 1308, 1546 and 1561 cm^{-1}.

Figure 16 The average background corrected spectra collected at 24 hours post mortem from the ovine _m. semimembranosus_ with the 5 lowest pH$_{24}$ values (5.44 – 5.48; grey) and the pHu values (5.59 – 5.61; black).

Tentative band assignments suggest that during the development of low pHu after 24 h there is a decrease in inorganic phosphate yet there is an increase in the concentration of the acidic form of phosphate evident in the decreased intensity at 582 cm^{-1} and increased intensity at 875 cm^{-1} (Movasaghi _et al._, 2007, Scheier _et al._, 2014). Lower pHu values also demonstrate increased α-helices (1308 cm^{-1}) and amide III (1278 cm^{-1}) protein bands as well as the breathing mode of nucleic acids including adenine (1255 cm^{-1}) and decreases in signals which have been related to COO$^-$ (1561 cm^{-1}) and NADH (1546 cm^{-1}) (Movasaghi _et al._, 2007). This suggests that between 24 hours and the development of pHu, the muscle is still undergoing anaerobic glycolysis and continued breakdown of ATP causing increased adenosine concentrations, decreased free NADH and changes to the structure of myofibrillar proteins as muscle contraction continues and actomyosin cross bridges continue to be made and broken (te Pas _et al._, 2004).

If it is hypothesised that an increase of intensities at 1334 and 1567 cm^{-1} in spectra from SMs with low pHu values are associated with higher concentrations of lactate as found by Scheier _et al._ (2014), the decrease in COO$^-$ signal between low pH$_{24}$ and low pHu values is surprising given that increases in lactate are correlated with continued anaerobic glycolysis (te Pas _et al._, 2004, Savell _et al._, 2005). To assign changes to spectra during the pre-rigor period, Scheier _et al._ (2014) collected reference Raman spectra of lactate that demonstrated it was characterised by peaks at 1334 cm^{-1} and 1567 cm^{-1}, which represent the CH group and COO$^-$ vibrations respectively. However, in comparing these reference signals to the Raman spectra collected from muscle, Scheier _et al._ (2014) may have over simplified the assignments as their study suggests excellent agreement

between spectra simulated from pure samples of metabolites and spectra measured from muscle, yet there is no consideration of the potential overlap in spectral contribution from other sources of CH group or COO^- vibrations, which are likely to be present in complex biological samples such as intact porcine muscle. A review of Raman spectroscopic studies conducted on biological tissues suggests that approximately 1560 – 1570 cm^{-1} Raman signals from tryptophan, tyrosine, amide II secondary protein structures and porphyrin may also contribute to the vibrations of COO^- (Movasaghi *et al.*, 2007) and it is plausible that metabolites that are closely related or have chemical conformations similar to lactate, such as pyruvate and acetate would also contribute to these spectral regions.

Therefore, the decrease in COO^- found in spectra characterising low pHu values may be a result of decreasing pyruvate. However, increasing concentrations of free H^+ with lower pHu values may result in free H^+ binding to other substrates, such as inorganic phosphate and lactate. If free H^+ binds to lactate creating lactic acid, the intensity of the COO^- would also be reduced, yet it is unclear whether lactate converts to lactic acid as literature on early post mortem events is unclear as authors use these terms interchangeably despite the differences in chemical conformation.

Furthermore, spectral signals from molecules with similar chemical conformation can be expected to overlap at wavelengths 1333 to 1335cm^{-1}, which represent the CH_2 and CH_3 vibrations because they are present in many biological compounds in muscle including hydroxyproline, a major component of collagen, nucleic acids and tryptophan (Movasaghi *et al.*, 2007). Given that it is difficult to obtain Raman spectra with low variation (Beattie *et al.*, 2004a) and no reference spectra or measurements were collected in this study, it is hard to justify strict assignment of bands, particularly since there were no SMs in the present study that deviate from the normal range pHu expected for lamb. Thus, more research is required to determine the chemical bonds that are contributing to the prediction of pHu and whether overlapping spectral assignments cause an over or under estimation for the prediction of meat quality traits resulting in lower predictability when cross validation methods are used.

Uncertainty of band assignments in Raman signals of complex samples also brings into question the validity of band assignments which have been completed in previous Raman spectroscopy studies aimed at predicting tenderness and sensory traits. Considering a broader number of Raman studies conducted on biological tissues, it is plausible that the spectral changes found by Beattie *et al.* (2008), Beattie *et al.* (2004b) and Schmidt *et al.* (2013) may relate to a broader number of biochemical characteristics of the meat. For example, it has been proposed that the intensity peak at approximately 930 – 940 cm^{-1} of α-helical protein structures is positively correlated with increasing tenderness (Schmidt *et al.*, 2013). While Pedersen *et al.* (2003) and Scheier *et al.* (2014) have associated increases at this peak with pH and glycogen levels, as well as protein conformations.

Therefore, it is hypothesised that the correlations between tenderness and Raman spectra may be an indirect measurement of the relationships between anaerobic glycolysis and pH decline (Savell *et al.*, 2005), pH decline, water holding capacity and tenderness (Tornberg, 1996, Huff Lonergan & Lonergan, 2005, Huff Lonergan *et al.*, 2010) and the relationships between myofibrillar structure and water holding capacity, tenderness and colour (Hughes *et al.*, 2014). Yet, this may be confounded by collagen content as the major components of collagen, such as tropocollagen, are

α-helical proteins which would also contribute to this band. Consequently, increases in the band associated with α-helical proteins could indicate a higher pHu through more glycogen present in muscle and therefore a greater water holding capacity or an increase in collagen which has been associated with decreases in tenderness (Purslow, 2005). In another Raman spectroscopic study, Beattie *et al.* (2004b) proposed that the changes in spectral region at approximately 1445 cm^{-1} are related to differences in the hydrophobicity of the proteins within the myofibril of beef silverside as there was a positive correlation with juiciness, sensory determination of tenderness and consumer acceptability and the intensity of this peak. However, other band assignments for this region indicate that the CH_2 and CH_3 groups of both collagen and lipids contribute to the Raman signals of this wavenumber (Movasaghi *et al.*, 2007). Therefore, it is plausible that the increases in juiciness, sensory tenderness and consumer acceptability could have been associated with increases in lipid content. As it is difficult to determine the exact biochemical and biophysical characteristics that are contributing the chemical bond vibrations and confounding relationships exist between meat quality traits, it may be a more useful approach to use Raman spectroscopy to predict a combination of meat quality traits of interest. Alternatively, Raman spectroscopy may provide a better prediction of meat sensory descriptors including tenderness, juiciness, flavour and overall liking as used in the Meat Standards Australia (MSA) grading systems (Thompson, 2002, Polkinghorne & Thompson, 2010) because these sensory properties are associated with more than one biochemical characteristic (Perry *et al.*, 2001).

3.2.4.3 Polyunsaturated Fatty Acids

As this is the first study assessing the Raman spectra of lipids in a complex matrix such as intact muscle, it isn't possible to assign the Raman spectral bands of FA composition with any certainty. However, a tentative interpretation is plausible based on FA composition studies using data from Raman spectroscopy research on adipose tissues (Beattie *et al.*, 2007, Lyndgaard *et al.*, 2011). These studies confirm that peaks in the intensity counts found in this research (Fig. 17) are typical of lipids, including the chemical bond vibrations of the C=O carbonyl stretch (1750cm^{-1}), the C=C and HC=CH stretches (1640 – 1650cm^{-1}), CH_2 twist and scissor (1300 and 1440cm^{-1}) and the C-C in phase and out of phase vibrations (1020 – 1130cm^{-1}). Although the signals are typical for FA composition of ruminant FAs (Beattie *et al.*, 2007), changes in FA composition generates shifts in the wavenumbers and the intensity counts of these key vibrations that provide information on the individual FAs present.
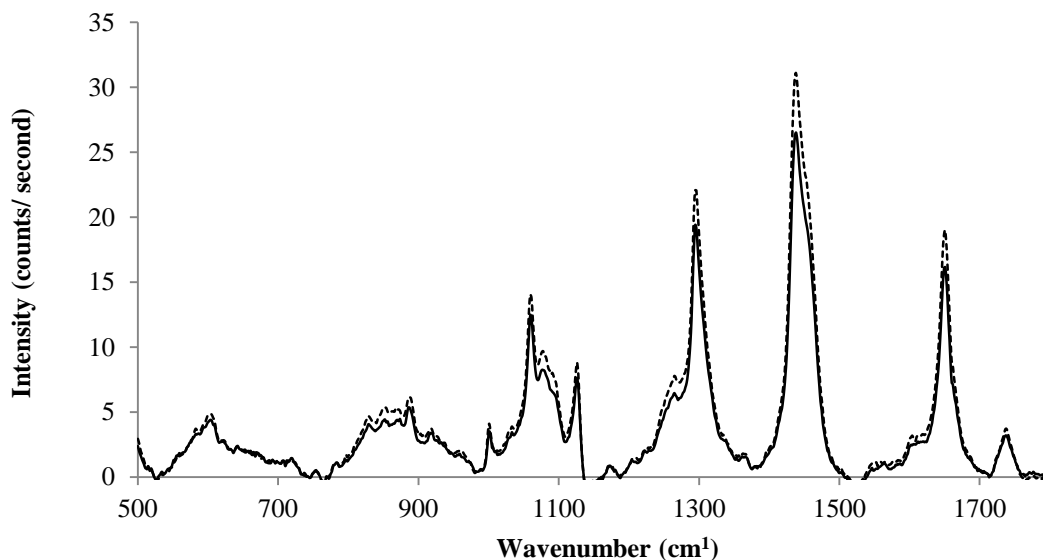

Figure 17. Baseline corrected, normalised and averaged Raman spectra of the five samples with the most PUFA (dotted line; 432.28 – 477.25 mg/100g meat) compared to the five samples with the lowest PUFA (black; 235.70 – 255.73 mg/100g meat).

Spectra collected from samples with high levels of PUFA demonstrated a 20% increase in intensity, as well as a shift of +3 cm^{-1} for the peak representing the C=C at approximately 1650 cm^{-1}. This is to be expected due to the chemical structure of FAs which have multiple unsaturated carbon – carbon bonds. Consequently, IMF containing higher amounts of PUFA also contains higher numbers of C=C bonds resulting in a positive correlation of this signal with increasing unsaturation. Consequently, this intensity peak dominates the spectra of lipids which are known to be high in PUFAs such as salmon and pork adipose tissues (Afseth *et al.*, 2006, Beattie *et al.*, 2007, Olsen *et al.*, 2007, Olsen *et al.*, 2010, Lyndgaard *et al.*, 2011).

The exact location of the C=C band is also important as it indicates the conformation of the C=C bonds (Lyndgaard *et al.*, 2011). Therefore the + 3 cm^{-1} shift evident in spectra from loins containing higher levels of PUFA may also suggest that the unsaturated FAs in these samples are comprised of more trans- bonds rather than cis-bonds, as the location of this band shifts to higher wavenumbers with increasing numbers of trans- bonds (Beattie *et al.*, 2004a, Lyndgaard *et al.*, 2011). This may be also linked to increasing PUFA and slight decreases in MUFA concentrations of these loins as shifts of this band to higher wavenumbers have also been associated with changes in composition from mono to polyunsaturated FAs in simple protein, fat and water emulsifications (Afseth *et al.*, 2005).

As the PUFA concentration consists of contributions from the cis- and trans- bonds of linoleic acid (C18: 2 n-6) (Nelson & Cox, 2008), the increasing contribution of PUFA's to the spectra may increase the contribution of trans- bonds. However, it is unlikely that it would be a significant shift, as overall there would still be a large contribution to this band from the concentration of oleic acid (C18:1(Δ⁹)), which has a similar chemical conformation and is present in a relatively high concentration as it is one of the main FAs found in lamb. This also highlights the difficulty in predicting FAs in complex mixtures because as RS relies on structural differences, it is unable to discriminate between PUFAs and MUFAs which have similar chemical structures.

Although peak intensities and locations of bands are important in determining the chemical composition of IMF, previous Raman spectroscopic research on lipids suggests that ratios between key intensity peaks cannot be over looked (Bresson *et al.*, 2005). One such example is the ratio of the C=C bond peak intensity to the C=O bond peak intensity at 1740 cm^{-1}. While spectra collected indicate that there is little difference in the C=O peak intensity between samples of different PUFA concentrations, changes to the C=C peak height at 1650 cm^{-1} indicates that a difference in the C=C:C=O ratio is evident as PUFA levels increase. Whilst previous studies on pork (Olsen *et al.*, 2007, Olsen *et al.*, 2010) and salmon (Afseth *et al.*, 2006) have used this ratio as an excellent indicator of the unsaturation of fats, this is not possible for this data set, since this ratio characterises the molal unsaturation rather than the mass unsaturation. This is due to the differences between mass and molal unsaturation, as mass unsaturation depends on the number of double bonds as well as the number of carbon chains per gram of sample (Beattie *et al.*, 2004a), which are not consistent between samples of this study due to the measurement of IMF rather than subcutaneous adipose tissue. Consequently, this ratio is a better indicator of iodine value rather than absolute amounts of unsaturated FAs. While a more accurate prediction of molal unsaturation may be achieved using Raman spectra, unlike pork manufacturing processes where iodine value has implications for fat firmness and product acceptability (Wood *et al.*, 2004), the prediction of iodine value has no benefit to the sheep meat industry.

Determination of the degree of unsaturation of FAs using Raman spectra is not only limited to the number of C=C bonds present. An 18% increase in the intensity peak at 1260 cm^{-1} that represents the C-H deformation is also evident in loins with higher amounts of PUFA. This agrees with the studies conducted by Afseth *et al.* (2006) and Lyndgaard *et al.* (2011) that have positively correlated increases in this peak with increasing concentrations of PUFA due to the CH deformation vibration which characterises the unsaturation of carbon- carbon chains. Given that this band decreases with increasing contributions from SFAs (Lyndgaard *et al.*, 2011), particularly C16:0 (Beattie *et al.*, 2004a), it is unsurprising that this band does not dominate the spectra as has previously been described by Lyndgaard *et al.* (2011) as lamb IMF contains more SFAs than pork adipose tissue (Wood *et al.*, 2008).

It is interesting to note that while spectra from loins with higher levels of PUFA demonstrate increased intensities for the peaks relating to unsaturation, there is also an increase in the Raman intensity of peaks which characterise SFAs. This is evident with a 10% increase at the C-C out of phase vibration at 1059 cm^{-1}, an 8% increase in the CH$_2$ twist vibration at 1290 cm^{-1} and a 15% increase and a + 3 cm^{-1} shift in the CH$_2$ scissor vibration at 1438 cm^{-1}. The increase of intensities at these wavenumbers suggests that the loins which are high in PUFA are also high in SFA as increasing intensity and decreasing width of these bands has been positively correlated with increasing levels of saturation (Beattie *et al.*, 2004a, Afseth *et al.*, 2006, Lyndgaard *et al.*, 2011).

Although chain length elicits an effect on the height and width of peak intensities (Beattie *et al.*, 2004a), it is unlikely that this is the cause of variation in spectra since lamb IMF is comprised of mostly medium chain FAs (carbon chain length between 12 – 20) and Raman signals remain constant with carbon chain lengths between 13 - 24 (Beattie *et al.*, 2004a). Temperature also has an effect on the Raman spectra as these bands broaden and decrease in intensities as FAs approach melting point (Beattie *et al.*, 2004a, Lyndgaard *et al.*, 2011). Although as Raman measurements were completed on loins at the same temperature it is unlikely that state of the lipids will account

for the variation.

Despite findings from previous Raman spectroscopic research on simple lipids being applied to studies on porcine subcutaneous adipose tissue with excellent predictive power (Olsen *et al.*, 2007, Olsen *et al.*, 2010), it is unclear what impact the measurement of fat within the muscle has on the Raman spectra. Since the lipids of adipose tissues are mainly triglycerides (Christie, 2012) which consist of three FAs each in an ester linkage with a single glycerol (Nelson & Cox, 2008) by measuring a constant amount of adipose tissue, changes to the concentration of any one FA category would alter the overall proportion of all the FA categories. As a result of this chemical structure, it is possible to directly relate CH_2 group vibrations to the number of saturated bonds and the C=O bonds to the number of FA side chains present. Saturated and unsaturated FA side chains in triglycerides are distinguishable because each C=C bond present in unsaturated FA removes 2 positions in the chain where carbon can bond to hydrogen atoms (Beattie *et al.*, 2004a). Therefore, at similar chain lengths SFA have more CH_2 groups compared to MUFA and PUFA.

Despite Afseth *et al.* (2006) proposing that in complex fat systems RS is unable to distinguish between MUFA and PUFA which have similar conformation when FAs are measured in the muscle of salmon, this may not be the case for the previous studies that have measured adipose tissue as it consists of only triglycerides. Due to the difference in the configuration of the C=C bonds in MUFA and PUFA, there are differences in the numbers of consecutive C-C bonds in the FA chain, as the C-C chain is 'broken' by C=C bonds. This means that while chemically similar FAs may contain the same number of C-C and C=C bonds, such as both α- linolenic acid (C18:2 n- 3) and γ- linolenic acid (C18:3 n- 6) that contain 14 C-C bonds and 3 C=C bonds, differences in the position of the C=C bonds along the chain results in consecutive chains of C-C bonds with different lengths. Thus, α-linolenic acid (C18:2 n- 3) has consecutive chains of C-C bonds of 8, 2, 2 and 2, while γ- linolenic acid has consecutive chains of C-C bonds of 5, 2, 2 and 5.

Beattie *et al.* (2004a) refer to this as the "apparent" chain length because Raman spectra reflect the number of consecutive C-C bonds rather than the absolute number of C-C bonds. Thus, consecutive chains of C-C bonds between C=C bonds within the hydrocarbon tails of MUFA and PUFA are characterised in spectra as separate shorter C-C chains. Due to the chemical structure of triglycerides with mixed FA of similar chain lengths such as pork adipose tissue, increasing concentrations of PUFA would reduce these "apparent" chain lengths per FA chain reflected in spectra more than increasing MUFA concentrations. Consequently, discrimination and better predictions of both MUFA and PUFA could be possible for triglycerides measured in adipose tissue as decreasing chain lengths per FA chain would be evident in the comparison of the C-C vibration to the carboxyl group (C=O) vibration at approximately 1740 cm^{-1}.

Conclusion

Interpretation of the spectra which underlies the predictions of meat quality traits and fatty acid composition highlights the complexity of Raman spectra collected from intact lamb muscles. Elucidating underlying spectra from the predictions of meat quality characteristics revealed that samples with high and low purge and pH values were discriminated using a variety of Raman signals pertaining to metabolic substrates. These included those which characterise phosphate (875 cm[1] and 1042 cm[1]), lactate (1334 cm[1] and 1567 cm[1]), α – helical proteins (937 cm[1]) and the amino acid

side chain vibrations (520 – 720 cm^1). However, these findings are limited to this study and further work is required to determine the impact of overlapping spectral signals from chemically similar compounds.

Direct comparison of Raman spectra from the prediction of fatty acid composition demonstrated that higher concentrations of PUFA were correlated with intensity peaks that correspond to the unsaturated C=C bonds at 1650 cm^{-1} and the CH deformation at 1260 cm^{-1}. Yet these spectra from LL portions with higher concentrations of PUFA also contained stronger signals for the CH$_2$ group and C-C vibrations which are associated with increasing saturation. Therefore, it is difficult to determine the influence on the predictions from overlapping spectral signals that arise from the measurement of FA chains in the phospholipid and triglyceride fractions that are measured in IMF within fresh intact muscle *in-situ*. The impact of correlations between IMF levels, FA composition and lipid fraction proportions on the prediction of FA composition using Raman spectroscopy is yet to be determined and future research will need to address this.

3.3 Success in meeting objectives

Experiments conducted between 2012 and 2014 successfully evaluated the potential of the Raman hand held probe to predict shear force values using spectra measured at 1 and 5 days post mortem to meet objectives 1 and 2. Additional research conducted as a component of experiments 1 and 5 also investigated the potential of the probe to predict fatty acid composition and intramuscular fat and all indicators of meat quality measured, therefore meeting objective 3 in regards to the potential to measure other meat quality traits. Spectra from models showing promise were background corrected and interpreted thereby establishing the biochemical and biophysical characteristics associated with the predictions made by the Raman hand held device successfully meeting the further requirements of objective 3.

3.4 Recommendations to Industry

Based on the findings presented here it is suggested that in its current state the Raman spectroscopic hand held device is unable to meet the industry requirements to provide a repeatable and robust prediction of shear force using spectra measured at either 1 or 5 days post mortem. However, with further development and improvement of electronic components it possible that this Raman spectroscopy is capable of predicting sensory properties (e.g. tenderness). This is plausible as sensory attributes are associated with more than one biochemical characteristic and therefore may not be negatively affected by the overlap of spectral features from chemically similar compounds.

Furthermore, the results presented in this report also indicate that there is potential to predict pH, purge and *L** values which are meat quality traits that relate to metabolic processes. Consequently, it may be possible to identify carcasses which deviate from normal post mortem metabolic processes, resulting in increased purge or low pHu values, using a single non-invasive measurement.

Using Raman spectroscopy to predict carcasses susceptible to high purge early post mortem could be beneficial to sheep meat processors, providing them with a decision making tool to determine

carcase suitability for chilled export markets. Yet there may be greater benefits from applying this technology to the beef industry where carcasses are more susceptible to deviations in pH/temperature decline and pHu values. Consequently, it may be possible to determine beef carcasses susceptible to dark firm and dry (DFD) as well as pale soft and exudative (PSE) characteristics using Raman spectroscopy. However, further development and validation of the technology is required to ensure it is robust enough to provide predictions which are repeatable long term in the extreme conditions required for online measurement. Furthermore, future research needs to determine whether the findings of this project transfer to other species or muscles. In this area with availability of the probe in June/July this year, an experiment was undertaken on beef muscle and the results of this will be reported separately, given the timelines for the current project.

3.5 Acknowledgements

3.6 Bibliography

Afseth, N. K., Segtnan, V. H., Marquardt, B. J. & Wold, J. P. (2005). Raman and near-infrared spectroscopy for quantification of fat composition in a complex food model system. *Applied Spectroscopy,* **59**, 1324 - 1332.

Afseth, N. K., Wold, J. P. & Segtnan, V. (2006). The potential of raman spectroscopy for characterisation of the fatty acid unsaturation of salmon. *Analytica Chimica Acta,* **572**, 85-92.

Anonymous (2005). *Handbook of australian meat,* Brisbane, Australia, AUS-MEAT Limited.

AOAC 1992. Aoac official method 991.36 fat (crude) in meat and meat products.

AOAC 2000. Aoac official methods of analysis. *AOAC Official Method 990.26.*

Arlot, S. & Celisse, A. (2010). A survey of cross validation procedures for model selection. *Statistics Survey,* **4**, 40 - 79.

Bauer, A., Agarkov, N., Scheier, R., Eberle, T., Pabst, M. & Schmidt, H. 2013. Evaluation of the tenderness of aged bovine gluetus medius muscles using raman spectroscopy and shear force measurements. *Proceedings of the 59th International Conference of Meat Science and Technology.* Izmir, Turkey.

Beattie, J., Bell, S. & Moss, B. (2004a). A critical evaluation of raman spectroscopy for the analysis of lipids: Fatty acid methyl esters. *Lipids,* **39**, 407-419.

Beattie, J. R., Bell, S. E. J., Borggaard, C. & Moss, B. W. (2008). Preliminary investigations on the effects of ageing and cooking on the raman spectra of porcine longissimus dorsi. *Meat Science,* **80**, 1205-1211.

Beattie, J. R., Bell, S. J., Borggaard, C., Fearon, A. & Moss, B. (2007). Classification of adipose tissue species using raman spectroscopy. *Lipids,* **42**, 679-685.

Beattie, J. R., Bell, S. J., Farmer, L. J., Moss, B. W. & Patterson, D. (2004b). Preliminary investigation of the application of raman spectroscopy to the prediction of the sensory quality of beef silverside. *Meat Science,* **66**, 903-913.

Bekhit, A. E. D., Farouk, M. M., Cassidy, L. & Gilbert, K. V. (2007). Effects of rigour temperature and electrical stimulation on venison quality. *Meat Science,* **75**, 564- 574.

Bonnier, F. & Byrne, H. J. (2012). Understanding the molecular information contained in principal component analysis of vibrational spectra of biological systems. *Analyst,* **137**, 322-332.

Bouton, P. E., Harris, P. V. & Shorthose, W. R. (1971). Effect of ultimate ph upon the water holding capacity and tenderness of mutton. *Journal of Food Science,* **36**, 435-439.

Bouton, P. E., Harris, P. V., Shorthose, W. R. & Baxter, R. I. (1973). Comparison of the effects of aging, conditioning and skeletal restraint on the tenderness of mutton. *Journal of Food Science,* **38**.

Bresson, S., Marssi, M. E. & Khelifa, B. (2005). Raman spectroscopy investigation of various saturated monoacid triglycerides. *Chemistry and Physics of Lipids,* **134**, 119-129.

Brøndum, J., Byrne, D. V., Bak, L. S., Bertelsen, G. & Engelsen, S. B. (2000). Warmed-over flavour in porcine meat — a combined spectroscopic, sensory and chemometric study. *Meat Science,* **54**, 83-95.

Bunow, M. R. & Levin, I. W. (1977). Comment on the carbon-hydrogen stretching region of vibrational raman spectra of phospholipids. *Biochimica et Biophysica Acta (BBA) - Lipids and Lipid Metabolism,* **487**, 388-394.

Choe, J. H., Choi, Y. M., Lee, S. H., Shin, H. G., Ryu, Y. C., Hong, K. C. & Kim, B. C. (2008). The relation between glycogen, lactate content and muscle fiber type composition, and their influence on postmortem glycolytic rate and pork quality. *Meat Science,* **80**, 355-362.

Choe, J. H. & Kim, B. C. (2014). Association of blood glucose, blood lactate, serum cortisol levels, muscle metabolites, muscle fiber type composition, and pork quality traits. *Meat Science,* **97**, 137-142.

Christie, W. W. 2012. Lipid compositions of animal tissues. *Lipid Library.* P.J. Barnes & Associates (The Oily Press).

Clayton, E. H., Gulliver, C. E., Piltz, J. W., Taylor, R. D., Blake, R. J. & Meyer, R. G. (2012). Improved extraction of saturated fatty acids but not omega-3 fatty acids from sheep red blood cells using a one-step extraction procedure. *Lipids,* **47**, 719-727.

Damez, J.-L. & Clerjon, S. (2008). Meat quality assessment using biophysical methods related to meat structure. *Meat Science,* **80**, 132-149.

Das, R. S. & Agrawal, Y. K. (2011). Raman spectroscopy: Recent advancements, techniques and applications. *Vibrational Spectroscopy,* **57**, 163-176.

Davies, A. M. & Fearn, T. (2006). Back to basics: Calibration statistics. *Spectroscopy Europe,* **18**, 31-32.

Dransfield, E., Etherington, D. J. & Taylor, M. A. J. (1992). Modelling post-mortem tenderisation—ii: Enzyme changes during storage of electrically stimulated and non-stimulated beef. *Meat Science,* **31**, 75-84.

England, E. M., Scheffler, T. L., Kasten, S. C., Matarneh, S. K. & Gerrard, D. E. (2013). Exploring the unknowns involved in the transformation of muscle to meat. *Meat Science,* **95**, 837-843.

Folch, J., Lees, M. & Sloane Stanley, G. H. (1957). A simple method for the isolation and purification of total lipids from animal tissues. *Journal of Biological Chemistry,* **226**, 497- 509.

Food Standards Australia New Zealand 2012. Nutrition information user guide.

Fowler, S. M., Schmidt, H., van de Ven, R., Wynn, P. & Hopkins, D. L. (2014a). Predicting tenderness of fresh ovine semimembranosus using raman spectroscopy. *Meat Science,* **97**, 597 - 601.

Fowler, S. M., Schmidt, H., van de Ven, R., Wynn, P. & Hopkins, D. L. (2014b). Raman spectroscopy compared against traditional predictors of shear force in lamb m. Longissimus lumborum. *Meat Science,* **98**, 652-656.

Geesink, G. H., Sujang, S. & Koohmaraie, M. (2011). Tenderness of pre- and post rigor lamb longissimus muscle. *Meat Science,* **88**, 723-726.

Hastie, T., Tishirani, R. & Friedman, J. 2008. The elements of statistical learning. Data mining, inference, and prediction 2nd ed.

Hedrick, H. B., Aberle, E. D., Forrest, J. C., Judge, M. D. & Merkel, R. A. (1993). *Principles of meat science*, Kendall Hunt Publishing Corporation.

Hernández, P., Navarro, J. L. & Toldrá, F. (1998). Lipid composition and lipolytic enzyme activities in porcine skeletal muscles with different oxidative pattern. *Meat Science,* **49**, 1-10.

Herrero, A. M. (2008a). Raman spectroscopy a promising technique for quality assessment of meat and fish: A review. *Food Chemistry,* **107**, 1642-1651.

Herrero, A. M. (2008b). Raman spectroscopy for monitoring protein structure in muscle food systems. *Critical Reviews in Food Science and Nutrition,* **48**, 512-523.

Hood, D. E. & Tarrant, P. V. (1981). *The problem of dark-cutting in beef,* The Netherlands, Martinus Nijhoff Publishers.

Hopkins, D. L., Allingham, P. G., Colgrave, M. & van de Ven, R. J. (2013). Interrelationship between measures of collagen, compression, shear force and tenderness. *Meat Science,* **95**, 219-223.

Hopkins, D. L. & Fogarty, N. M. (1998). Diverse lamb genotypes—2. Meat ph, colour and tenderness. *Meat Science,* **49**, 477-488.

Hopkins, D. L., Hegarty, R. S., Walker, P. J. & Pethick, D. W. (2006). Relationship between animal age, intramuscular fat, cooking loss, ph, shear force and eating quality of aged meat from young sheep. *Australian Journal of Experimental Agriculture,* **46**, 879-884.

Hopkins, D. L., Kerr, M. J., Kerr, M. G. & van de Ven, R. 2012. Within sample variance for shear force testing of lamb meat. *Proceedings of the 29th Biennial Conference of the Australian Society of Animal Production.* Christchurch, New Zealand.

Hopkins, D. L., Kerr, M. J. & van de Ven, R. Within sample variance for particle size testing of red meat. . Proceedings of the 30th Biennial Conference of the Australian Society of Animal Production, 2014. 55.

Hopkins, D. L., Stanley, D. F., Toohey, E. S., Gardner, G. E., Pethick, D. W. & van de Ven, R. (2007). Sire and growth path effects on sheep meat production 2. Meat and eating quality. *Australian Journal of Experimental Agriculture,* **47**, 1219-1228.

Hopkins, D. L. & Thompson, J. M. (2002). Factors contributing to proteolysis and disruption of myofibrillar proteins and the impact on tenderisation in beef and sheep meat. *Australian Journal of Agricultural Research,* **53**, 149-166.

Hopkins, D. L., Toohey, E. S., Kerr, M. J. & van de Ven, R. (2011a). Comparison of two instruments (g2 tenderometer and a lloyd texture analyser) for measuring the shear force of cooked meat. *Animal Production Science,* **51**, 71-76.

Hopkins, D. L., Toohey, E. S., Lamb, T. A., Kerr, M. J., van de Ven, R. & Refshauge, G. (2011b). Explaining the variation in the shear force of lamb meat using sarcomere length, the rate of rigor onset and ph. *Meat Science,* **88**, 794-796.

Huff Lonergan, E. & Lonergan, S. M. (2005). Mechanisms of water holding capacity: The role of post mortem biochemical and structural changes. *Meat Science,* **71**, 194 - 204.

Huff Lonergan, E., Zhang, W. & Lonergan, S. M. (2010). Biochemistry of postmortem muscle — lessons on mechanisms of meat tenderization. *Meat Science,* **86**, 184-195.

Hughes, J. M., Oiseth, S. K., Purslow, P. P. & Warner, R. D. (2014). A structural approach to understanding the interactions between colour, water-holding capacity and tenderness. *Meat Science,* **98**, 520-532.

Hwang, I. H., Devine, C. E. & Hopkins, D. L. (2003). The biochemical and physical effects of electrical stimulation on beef and sheep meat tenderness. *Meat Science,* **65**, 677-691.

Hwang, I. H., Park, B. Y., Cho, S. H. & Lee, J. M. (2004). Effects of muscle shortening and proteolysis on warner–bratzler shear force in beef longissimus and semitendinosus. *Meat Science,* **68**, 497-505.

Karumendu, L. U., van de Ven, R., Kerr, M. J., Lanza, M. & Hopkins, D. L. (2009). Particle size analysis of lamb meat: Effect of homogenization speed, comparison with myofibrillar fragmentation index and its relationship with shear force. *Meat Science,* **82**, 425-431.

Kerth, C. R. (2013). *The science of meat quality,* Hoboken, Wiley.

Khliji, S., van de Ven, R., Lamb, T. A., Lanza, M. & Hopkins, D. L. (2010). Relationship between consumer ranking of lamb colour and objective measures of colour. *Meat Science,* **85**, 224-229.

Klont, R. E., Brocks, L. & Eikelenboom, G. (1998). Muscle fibre type and meat quality. *Meat Science,* **49, Supplement 1**, S219-S229.

Koohmaraie, M. & Geesink, G. H. (2006). Contribution of postmortem muscle biochemistry to the delivery of consistent meat quality with particular focus on the calpain system. *Meat Science,* **74**, 34-43.

Koohmaraie, M., Seideman, S. C. & Crouse, J. D. (1988). Effect of subcutaneous fat and high temperature conditioning on bovine meat tenderness. *Meat Science,* **23**, 99-109.

Larsson, K. & Rand, R. P. (1973). Detection of changes in the environment of hydrocarbon chains by raman spectroscopy and its application to lipid-protein systems. *Biochimica et Biophysica Acta (BBA) - Lipids and Lipid Metabolism,* **326**, 245-255.

Lee, M. S., Apple, J. K., Yancey, J. W. S., Sawyer, J. T. & Johnson, Z. B. (2008). Influence of vacuum-aging period on bloom development of the beef gluteus medius from top sirloin butts. *Meat Science,* **80**, 592-598.

Li-Chan, E. C. Y., Nakai, S. & Hirotsuka, M. (1994). Raman spectroscopy as a probe of protein structure in food systems. *In:* YADA, R. Y., JACKMAN, R. L. & SMITH, J. L. (eds.) *Protein structure- function relationships in food.* Glasgow, NZ: Blackie Academic and Professional

Lis, L. J., Goheen, S. C., Kauffman, J. W. & Shriver, D. F. (1976). Laser raman spectroscopy of lipid-protein systems differences in the effect of intrinsic and extrinsic proteins on the phosphatidylcholine raman spectrum. *Biochimica et Biophysica Acta (BBA) - Nucleic Acids and Protein Synthesis,* **443**, 331-338.

Lyndgaard, L. B., Sorensen, K. M., van den Berg, F. & Engelsen, S. B. (2011). Depth profiling of porcine adipose tissue by raman spectroscopy. *Journal of Raman Spectroscopy,* **43**, 482-489.

Matousek, P. & Stone, N. (2009). Emerging concepts in deep raman spectroscopy of biological tissue. *Analyst,* **134**, 1058-1066.

McCreery, R. L. 2000. Raman spectroscopy for chemical analysis. *In:* WINEFORDNER, J. D. (ed.) *A Series of Monographs of Analytical Chemistry and it's Applications.* New York, USA: Wiley-Interscience John Wiley & Sons Inc.

McCreery, R. L. 2005. Raman spectroscopy for chemical analysis. 1 ed. Hoboken: Wiley-Interscience.

Melody, J. L., Lonergan, S. M., Rowe, L. J., Huiatt, T. W., Mayes, M. S. & Huff-Lonergan, E. (2004). Early postmortem biochemical factors influence tenderness and water-holding capacity of three porcine muscles. *Journal of Animal Science,* **82**, 1195-1205.

Mevik, B. H., Wehrens, R. & Liland, K. H. 2011. Pls: Partial least squares and principal component regression. *In:* R PACKAGE (ed.). version 2.3-0.

Movasaghi, Z., Rehman, S. & Rehman, I. U. (2007). Raman spectroscopy of biological tissues. *Applied Spectroscopy Reviews,* **42**, 493-541.

Nakamura, Y. N., Tsuneishi, E., Kamiya, M. & Yamada, A. (2010). Histological contribution of collagen architecture to beef toughness. *Journal of Food Science,* **75**, E73-E77.

Nelson, D. L. & Cox, M. M. (2008). *Principles of biochemistry,* New York, USA, Freeman and Company.

Olsen, E. F., Baustad, C., Egelandsdal, B., Rukke, E.-O. & Isaksson, T. (2010). Long-term stability of a raman instrument determining iodine value in pork adipose tissue. *Meat Science,* **85**, 1-6.

Olsen, E. F., Rukke, E.-O., Flåtten, A. & Isaksson, T. (2007). Quantitative determination of saturated-, monounsaturated- and polyunsaturated fatty acids in pork adipose tissue with non-destructive raman spectroscopy. *Meat Science,* **76**, 628-634.

Ouali, A. (1992). Proteolytic and physicochemical mechanisms involved in meat texture development. *Biochimie,* **74**, 251-265.

Ouali, A., Herrera-Mendez, C. H., Coulis, G., Becila, S., Boudjellal, A., Aubry, L. & Sentandreu, M. A. (2006). Revisiting the conversion of muscle into meat and the underlying mechanisms. *Meat Science,* **74**, 44-58.

Pannier, L., Gardner, G. E., Pearce, K. L., McDonagh, M., Ball, A. J., Jacob, R. H. & Pethick, D. W. (2014). Associations of sire estimated breeding values and objective meat quality measurements with sensory scores in australian lamb. *Meat Science,* **96**, 1076-1087.

Pearce, K. L., Rosenvold, K., Andersen, H. J. & Hopkins, D. L. (2011). Water distribution and mobility in meat during the conversion of muscle to meat and ageing and the impacts on fresh meat quality attributes — a review. *Meat Science,* **89**, 111-124.

Pedersen, D. K., Morel, S., Andersen, H. J. & Balling Engelsen, S. (2003). Early prediction of water-holding capacity in meat by multivariate vibrational spectroscopy. *Meat Science,* **65**, 581-592.

Perry, D., Thompson, J. M., Hwang, I. H., Butchers, A. & Egan, A. F. (2001). Relationship between objective measurements and taste panel assessment of beef quality. *Australian Journal of Experimental Agriculture,* **41**, 981-989.

Pézolet, M., Pigeon, M., Ménard, D. & Caillé, J. P. (1988). Raman spectroscopy of cytoplasmic muscle fiber proteins. Orientational order. *Biophysical Journal,* **53**, 319-325.

Polkinghorne, R. J. & Thompson, J. M. (2010). Meat standards and grading: A world view. *Meat Science,* **86**, 227-235.

Ponnampalam, E. N., Butler, K. L., Pearce, K. M., Mortimer, S. I., Pethick, D. W., Ball, A. J. & Hopkins, D. L. (2014). Sources of variation of health claimable long chain omega-3 fatty acids in meat from australian lamb slaughtered at similar weights. *Meat Science,* **96**, 1095-1103.

Ponnampalam, E. N., Sinclairt, A. J., Egan, A. R., Blakeley, S. J. & Leury, B. J. (2001a). Effect of diets containing n-3 fatty acids on muscle long-chain n-3 fatty acid content in lambs fed low- and medium-quality roughage diets. *Journal of Animal Science,* **79**, 698-706.

Ponnampalam, E. N., Trout, G. R., Sinclair, A. J., Egan, A. R. & Leury, B. J. (2001b). Comparison of the color stability and lipid oxidative stability of fresh and vacuum packaged lamb muscle containing elevated omega-3 and omega-6 fatty acid levels from dietary manipulation. *Meat Science,* **58**, 151-161.

Priolo, A., Micol, D. & Agabriel, J. (2001). Effects of grass feeding systems on ruminant meat colour and flavour. A review. *Animal Research,* **50**, 185-200.

Puolanne, E. & Halonen, M. (2010). Theoretical aspects of water-holding in meat. *Meat Science,* **86**, 151-165.

Purslow, P. P. (2005). Intramuscular connective tissue and its role in meat quality. *Meat Science,* **70**, 435-447.

R Core Team 2013. R: A language and environment for statistical computing. *In:* R FOUNDATION FOR STATISTICAL COMPUTING (ed.). Vienna, Austria.

Savell, J. W., Mueller, S. L. & Baird, B. E. (2005). The chilling of carcasses: A review. *Meat Science,* **70**, 449- 459.

Scheffler, T. L., Scheffler, J. M., Kasten, S. C., Sosnicki, A. A. & Gerrard, D. E. (2013). High glycolytic potential does not predict low ultimate ph in pork. *Meat Science,* **95**, 85-91.

Scheier, R., Köhler, J. & Schmidt, H. (2014). Identification of the early post mortem metabolic state of porcine m. Semimembranosus using raman spectroscopy. *Vibrational Spectroscopy,* **70**, 12 -17.

Scheier, R. & Schmidt, H. (2013). Measurement of the ph value in pork meat early postmortem by raman spectroscopy. *Applied Physics B,* **111**, 289-297.

Schmidt, H., Scheier, R. & Hopkins, D. L. (2013). Preliminary investigation on the relationship of raman spectra of sheep meat with shear force and cooking loss. *Meat Science,* **93**, 138-143.

Schmidt, H., Sowoidnich, K. & Kronfeldt, H. D. (2010). A prototype hand-held raman sensor for the in situ characterization of meat quality. *Applied Spectroscopy,* **64**, 888-894.

Schmidt, H., Sowoidnich, K., Maiwald, M., Sumpf, B. & Kronfeldt, H. D. Hand-held raman sensor head for *in-situ* characterization of meat quality applying a mircosystem 671nm diode laser. *In:* VO-DINH, T., LIEBERMAN, R. A. & GAUGLITZ, G., eds. Proc Advan Environ, Chem and Bio Sensing Tech VI, 2009 Orlando, Florida, United States. International Society for Optics and Photonics, 1-8.

Sikorski, Z. E. (1978). Protein changes in muscle foods due to freezing and frozen storage. *International Journal of Refrigeration,* **1**, 173- 180.

Smulders, F. J. M., Marsh, B. B., Swartz, D. R., Russell, R. L. & Hoenecke, M. E. (1990). Beef tenderness and sarcomere length. *Meat Science,* **28**, 349-363.

Susi, H., Sampungna, J., Hampson, J. W. & Ard, J. S. (1979). Laser-raman investigation of phospholipid- polypeptide interactions in model membranes. *Biochemistry,* **18**, 297-.

Takahashi, K. (1996). Structural weakening of skeletal muscle tissue during post-mortem ageing of meat: The non-enzymatic mechanism of meat tenderization. *Meat Science,* **43, Supplement 1**, 67-80.

Taylor, R. & Frylinck, L. 2003. Muscle structures which determine meat tenderness in south african and other beef breeds. *Consistency of Quality- 11th International Meat Symposium.*

te Pas, M. F. W., Everts, M. E. & Haagsman, H. P. (2004). *Muscle development of livestock animals- physiology, genetics and meat quality,* Oxfordshire, United Kingdom, CABI Publishing.

Thompson, J. M. (2002). Managing meat tenderness. *Meat Science,* **62**, 295-308.

Thompson, J. M., Gee, A., Hopkins, D. L., Pethick, D. W., Baud, S. R. & O'Halloran, W. J. (2005a). Development of a sensory protocol for testing palatability of sheep meats. *Australian Journal of Experimental Agriculture,* **45**, 469-476.

Thompson, J. M., Hopkins, D. L., D'Souza, D. N., Walker, P. J., Baud, S. R. & Pethick, D. W. (2005b). The impact of processing on sensory and objective measurements of sheep meat eating quality. *Australian Journal of Experimental Agriculture,* **45**, 561-573.

Toohey, E. S., Hopkins, D. L., Stanley, D. F. & Nielsen, S. G. (2008). The impact of new generation pre-dressing medium-voltage electrical stimulation on tenderness and colour stability in lamb meat. *Meat Science,* **79**, 683-691.

Tornberg, E. (1996). Biophysical aspects of meat tenderness. *Meat Science,* **43**, 175-191.

Wallach, D. F. H., Verma, S. P. & Fookson, J. (1979). Application of laser raman and infrared spectroscopy to the analysis of membrane structure. *Biochimica et Biophysica Acta (BBA) - Reviews on Biomembranes,* **559**, 153-208.

Wood, J. D., Enser, M., Fisher, A. V., Nute, G. R., Sheard, P. R., Richardson, R. I., Hughes, S. I. & Whittington, F. M. (2008). Fat deposition, fatty acid composition and meat quality: A review. *Meat Science,* **78**, 343-358.

Wood, J. D., Richardson, R. I., Nute, G. R., Fisher, A. V., Campo, M. M., Kasapidou, E., Sheard, P. R. & Enser, M. (2004). Effects of fatty acids on meat quality: A review. *Meat Science,* **66**, 21-32.

Yang, D. & Ying, Y. (2011). Applications of raman spectroscopy in agricultural products and food analysis: A review. *Applied Spectroscopy Reviews,* **46**, 539-560.

3.7 Press Articles

ABC Central West NSW (Orange) 20th May 2015- Radio Interview Rural Report

Cowra Guardian 24th April 2013- New tender test, with no need for old fashioned touching

The Land 28th February 2013- New tenderness test

ABC Central West NSW (Orange) 25th February 2013- Radio Interview 6.47 am

Country Leader Tamworth 25th February 2013- Probing lamb tenderness

North West Magazine Insert 25th February 2013- World- first portable laser lamb probe

2EL (Orange) 25th February 2013- Local Lunch Radio Interview 1.35 pm

Cowra Guardian 22nd February 2013- Laser probe could revolutionise industry

2MN (Mussellbrook) 21st February 2013- Radio Interview 6.35am

Forbes Advocate 21st February 2013- Leading way with lamb

Walcha News 21st February 2013- Laser lamb probe to test for tenderness

Media Release 20th February 2013- World First Portable laser lamb probe

3.8 Published Papers

Fowler, S.M, Schmidt, H., van de Ven, R., and Hopkins, D.L. (2015). Prediction of lamb meat quality using a Raman Spectroscopic hand held device, Proc 11th Australian Conference of Vibrational Spectroscopy/5th Asian Spectroscopy Conference, Sydney, NSW.

Fowler, S.M., Wood, B.R., Ottoboni, M., Baldi, G. Wynn, P. and Hopkins, D.L. (2015) Imaging of intact ovine *m. semimembranosus* by confocal Raman microscopy. Journal of Food and Bioprocess Technology. (In Press)

Fowler, S. M., Schmidt, H., van de Ven, R., Wynn, P. & Hopkins, D. L. (2015). Predicting meat quality traits of ovine m. Semimembranosus, both fresh and following freezing and thawing, using a hand held raman spectroscopic device. Meat Science*,* 108, 138-144.

Fowler, S. M., Ponnampalam, E. N., Schmidt, H., Wynn, P. & Hopkins, D. L. (2015). Prediction of intramuscular fat content and major fatty acid groups of lamb m. Longissimus lumborum using raman spectroscopy. Meat Science, 110, 70-75.

Fowler, S.M, Schmidt, H., van de Ven, R., Wynn, P.C. and Hopkins, D.L. (2014). Star wars lamb... can lasers measure meat quality? Proc CRC Annual Postgraduate Conference, p. 21. Sydney, NSW.

Fowler, S.M., Schmidt, H., Clayton, E.H., Bailes, K., Wynn, P., and Hopkins, D.L. (2014). Predicting fatty acid composition of ovine *longissimus thoracis lumborum* using Raman spectroscopy. Proceedings of the 30th Biennial Conference of the Australian Society of Animal Production, p54.

Fowler, S.M., Wood, B.R.., Ottoboni, M.., Baldi, G.., Wynn, P., and Hopkins, D.L. (2014). Imaging of intact ovine *semimembranosus* by confocal Raman microscopy. Proc. 60th International Congress of Meat Science and Technology. (Paper 69, pp. 1-4), Punta Del Este, Uruguay.

Fowler, S.M., Schmidt, H., Clayton, E.H., Bailes, K., Wynn, P., and Hopkins, D.L. (2014). Predicting fatty acid composition of lamb loin using Raman spectroscopy. Proc. 60th International Congress of Meat Science and Technology. (Paper 70, pp. 1-4), Punta Del Este, Uruguay.

Fowler, S.M., Schmidt, H., van de Ven, R., Wynn, P., and Hopkins, D.L. (2014). Raman Spectroscopy compared against traditional indicators of shear force in lamb *m. longissimus lumborum*. Meat Science, 98, 652-656.

Fowler, S.M., Schmidt, H., van de Ven, R., Wynn, P., and Hopkins, D.L. (2014). Predicting tenderness of fresh ovine semimembranosus using Raman spectroscopy. Meat Science, 97, 597-601.

Fowler, S., Schmidt, H., van de Ven, R., Wynn, P. and Hopkins, D. (2013). Predicting tenderness of fresh intact ovine *longissimus thoracis lumborum* using Raman Spectroscopy. Proc. 59th International Congress of Meat Science and Technology. S7B-5, pp 1-4, Izmir, Turkey.

Fowler, S., Schmidt, H., van de Ven, R., Wynn, P. and Hopkins, D. (2013). Predicting tenderness of fresh intact ovine semimembranosus using Raman Spectroscopy. Proc. 59th International Congress

of Meat Science and Technology. O-19, pp 1-4, Izmir, Turkey.

Schmidt, H., Fowler, S., Scheier, R., van de Ven, R., Wynn, P, and Hopkins, D.L. (2013). Correlation of Raman spectra of sheep meat with shear force – can we measure or predict toughness with an optical measurement? Proc. BIT's 2nd World Congress of Food Science and Technology, p 88, Hangzhou, China.

Fowler, S.M, Wood, B., Wynn, P. and Hopkins, D.L. (2013). Characterising tenderness of intact ovine semimembranosus using Raman Microscopy. Proc CRC Annual Postgraduate Conference, Coffs Harbour, NSW.